



Comparison of pesticide adsorption efficiencies of zeolites and zeolite-carbon composites and their regeneration possibilities

Magdalena Andrunik^{a, **}, Mateusz Skalny^a, Marta Gajewska^b, Mateusz Marzec^b, Tomasz Bajda^{a, *}

^a AGH University of Science and Technology, Faculty of Geology, Geophysics and Environmental Protection, A. Mickiewicz 30 Ave, 30-059, Krakow, Poland

^b AGH University of Science and Technology, Academic Centre for Materials and Nanotechnology, A. Mickiewicz 30 Ave, 30-059, Krakow, Poland

ARTICLE INFO

Keywords:

Surfactant
Modification
Fly-ash
Remediation
Organic compounds

ABSTRACT

The presence of pesticides in our environment is a consequence of intensive industrial and civilizational development, necessitating the search for effective and safe methods to remove them. We suggest utilizing zeolite X and a zeolite-carbon composite, obtained through the chemical transformation of fly ash, as pesticide sorbents. To increase the sorption efficiency of 2,4-dichlorophenoxyacetic acid (2,4-D), 2-methyl-4-chlorophenoxyacetic acid (MCPA), carbendazim, and simazine, we functionalized the zeolite materials with cationic (hexadecyltrimethylammonium) and nonionic (Triton X-100) surfactants. We used transmission electron microscopy (TEM), X-ray photoelectron spectroscopy (XPS), thermogravimetric/differential thermal analysis (TG/DTA) and point of zero charge (pHpzc) analysis to characterize the functionalized sorbent materials. Our results indicate that cationic surfactants significantly enhance the adsorption of 2,4-D and MCPA. In contrast, carbendazim and simazine exhibit maximum sorption on the unmodified zeolite-carbon composite. The sorption mechanism is intricate, with physical sorption predominating, primarily due to electrostatic interactions between the protonated binding sites of the adsorbents and the negatively charged pesticide molecules. Regeneration tests demonstrated that ethanol is the most effective in regenerating zeolite-carbon composite with adsorbed MCPA and 2,4-D, while thermal regeneration was not possible. Adsorbents with simazine and carbendazim can be regenerated using both thermal and ethanol methods, but the thermal regeneration of zeolite with adsorbed simazine is more efficient. Utilizing functionalized zeolite materials obtained from industrial waste, such as fly ash, could provide an efficient way to remove pesticides from the environment.

1. Introduction

The rapid expansion of the economy, urbanization, and the need to increase food production has led to persistent pollution of water. This has resulted in significant consequences for food quality and poses a considerable burden on public health and the environment, leading to severe damage to ecosystems as a consequence of the excessive and improper use of pesticides [1–5]. The term

* Corresponding author. AGH University of Science and Technology, al. Mickiewicza 30, 30-059, Krakow, Poland.

** Corresponding author. AGH University of Science and Technology, al. Mickiewicza 30, 30-059, Krakow, Poland.

E-mail addresses: andrunik@meeri.pl (M. Andrunik), bajda@agh.edu.pl (T. Bajda).

<https://doi.org/10.1016/j.heliyon.2023.e20572>

Received 2 June 2023; Received in revised form 20 September 2023; Accepted 29 September 2023

Available online 4 October 2023

2405-8440/© 2023 The Authors. Published by Elsevier Ltd. This is an open access article under the CC BY-NC-ND license (<http://creativecommons.org/licenses/by-nc-nd/4.0/>).

“pesticide” refers to any substance, whether chemical, biological, or otherwise, used to prevent, destroy, or control any species of plants or animals that interfere with desired plant growth and production, processing, storage, or transport. Unfortunately, most sprayed pesticides do not reach their intended target but rather spread through the air, water, and soil. This has led to the detection of trace amounts of these chemicals in surface water, and, even more critically, in groundwater, which is a vital source of drinking water on a global scale [6–9]. Moreover, while pesticides should ideally target only specific pests, most are broad-spectrum, meaning their effects cannot be limited to individual pests. This results in damage to beneficial organisms as well.

Pesticides can be classified based on their usage and potential to kill living organisms. Examples of pesticide types include insecticides, herbicides, rodenticides, fungicides, molluscicides, bactericides, avicides, virucides, algicides, acaricides, and miticides [10, 11]. They can also be categorized according to the chemical composition of their active ingredients. Pesticides are categorized into four chemical groups: organochlorines, organophosphorus, carbamates, and pyrethrins and pyrethroids. Besides these four primary groups, there are other miscellaneous pesticide groups like phenoxyacetic acid and bipyridyls. Another category comprises inorganic pesticides, which encompass compounds such as sulfur, copper, mercury, lead, and arsenic. These pesticides exhibit high persistence and have resulted in substantial soil pollution issues in certain regions [12].

There are three primary methods for removing pesticides from different matrices, depending on the remediation processes used: biological, chemical, and physical, where these last two are sometimes combined or used in a coordinated manner [13]. Chemical remediation involves the utilization of specific chemical agents to transform pesticides into either harmless or less harmful substances. This approach encompasses various advanced oxidation processes (AOPs), such as UV–H₂O₂ and UV–ozone treatment, as well as the photocatalysis, and photodegradation methods, ultrasound-assisted remediation, and the oxidation of organic substrates using Fe(II) and hydrogen peroxide [14–23]. Physical remediation methods include coagulation, membrane processes, and adsorption. Adsorption is among the most frequently employed techniques for water purification because of its effectiveness, capacity, and suitability for large-scale applications [3,24–31].

Materials derived from natural minerals or waste materials, serving as adsorbents for water purification, have garnered significant attention in recent years. Zeolites, primarily synthesized from kaolin clay, along with kaolin itself, have demonstrated successful applications as adsorbents for pollutant removal [32–34]. Nevertheless, the current focus of intensive research lies in exploring the potential of utilizing hard coal and lignite fly ashes in the synthesis of zeolite materials. On a global scale, the coal industry generates approximately 750 million tons of fly ashes each year. However, the rates of utilization of these fly ashes differ significantly among countries, with utilization ranging from 99% in Japan to as low as 11% in Africa and the Middle East [35]. The chemical composition of coal fly ash allows for efficient transformation into alternative materials like zeolites and zeolitic materials, making it a promising avenue for various applications [36–39]. The presence of aluminum and silicon in fly ash offers a valuable source of aluminosilicate for synthesizing zeolites and zeolitic materials [40–42].

Zeolite-based adsorbents possess unique physicochemical properties, are readily available, and have low costs. They are used extensively in agriculture, industry, and pollution control, specifically as adsorbents for removing heavy metals and pesticides [13,43, 44]. Carbon-based adsorbents are also gaining more attention as adsorbents of organic pollutants. Zeolite-carbon composites combine the unique properties of both materials and can be obtained in various forms such as fibers, cloths, discs, and monoliths, with high Brunauer–Emmett–Teller surface areas, large pore volumes, and stability at high temperatures and in a nonoxidizing atmosphere [45–47]. Furthermore, it has been shown that modifying the surface of zeolites with organic surfactants significantly enhances their adsorption properties for some pesticides. The proper choice of surfactants is crucial to increase the adsorption of various pollutants, as the surfactants’ structure and charge determine the further properties of the modified adsorbents. For instance, Arnnok and Burakham [48] provided evidence that surfactant-modified adsorbents are highly proficient in extracting carbamate pesticides. The adsorption rates for oxamyl, carbofuran, carbaryl, methiocarb, and carbosulfan exceeded 94% when employing cetyltrimethylammonium bromide-modified zeolite.

This study focuses on exploring a novel approach to address the issue of pesticide adsorption. The principal objective of this research is to conduct a comprehensive investigation into the efficacy of both modified and unmodified zeolites, as well as zeolite-carbon composites, in the adsorption of four distinct pesticides. These pesticides include 2-(2,4-dichlorophenoxy)acetic acid (2,4-D) and 2-(4-chloro-2-methylphenoxy)acetic acid (MCPA) belonging to the phenoxyacetic acid class, methyl N-(1H-benzimidazol-2-yl) carbamate (carbendazim) from the carbamate class, specifically benzimidazole, and 6-chloro-2-N,4-N-diethyl-1,3,5-triazine-2,4-diamine (simazine), which is classified as an organochloride within the triazine herbicide category. Zeolites and zeolite-carbon composites used for adsorption were modified using cationic and nonionic surfactants, and the modification was thoroughly examined in previous studies [49]. In this work, we analyzed the adsorption of the mentioned pesticides concerning the initial concentration, initial pH of the solution, kinetics, and competitive adsorption. We also determined the possibility of regenerating and reusing adsorbents and investigated the stability of adsorbents during the adsorption process. Notably, this work represents the first study on the effectiveness of fly ash-based and surfactant-modified zeolites and zeolite-carbon composites for adsorbing pesticides. Furthermore, it includes a comparative analysis of various approaches to regenerating adsorbents. In summary, the primary aim of this study was to gain insights into the mechanisms of pesticide adsorption and to evaluate the potential of fly ash-based and surfactant-modified zeolites and zeolite-carbon composites as highly effective adsorbents for pesticides. The outcomes of this investigation could have significant implications in addressing pesticide contamination and its impact on the environment and human health.

2. Materials and methods

2.1. Materials

In this research, two distinct adsorbents were employed: zeolite type X (referred to as X-FA) and a zeolite-carbon composite incorporating zeolite type X (referred to as X-C). These materials were derived from the conversion of fly ashes. Zeolite X was synthesized from F-class fly ash (FA) using the hydrothermal method [50], while the zeolite-carbon composite was created from high-carbon fly ash (HCFA) through a one-step hydrothermal conversion process [51]. The particle size of the zeolite and zeolite-carbon composite agglomerates ranged up to 100 μm , with a D50 value ranging between 21 and 32 μm . Both adsorbents were modified using various surfactants, namely hexadecyltrimethylammonium bromide (HDTMA-Br) and t-octylphenoxypolyethoxyethanol (Triton X-100, TX100). HDTMA-Br is composed of 19 ethylene molecules, compensated with Br⁻. In an aqueous solution, this salt dissociates into an organic cation (HDTMA) and an inorganic anion (Br⁻). For the modification of adsorbents, the cationic part of the surfactant (HDTMA) was utilized. The modification process was described extensively by Andrunik et al. [49]. To summarize, the zeolite and zeolite-carbon composite samples were mixed with either HDTMA or TX100 solutions, each at concentrations equivalent to 1.0 ECEC of the respective material. This mixing took place at 40 °C for a duration of 24 h. Subsequently, the samples were subjected to centrifugation for 10 min at 14,000 rpm, followed by decanting the supernatant. Finally, the samples were dried at 80 °C for a period of 24 h.

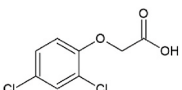
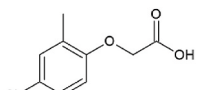
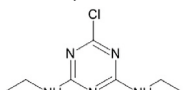
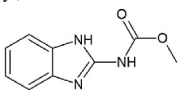
2.2. Adsorption study

For the experiments, four pesticides were selected, namely 2-(2,4-dichlorophenoxy)acetic acid (2,4-D), 2-(4-chloro-2-methylphenoxy)acetic acid (MCPA), 6-chloro-2-N,4-N-diethyl-1,3,5-triazine-2,4-diamine (simazine), and methyl N-(1H-benzimidazol-2-yl)carbamate (carbendazim) (Table 1).

In the adsorption experiments involving initial concentration variations, 20 mg of both unmodified and modified adsorbents were placed into separate test tubes. Then, 5 ml of pesticide solutions with different concentrations were introduced into the test tubes. For 2,4-D and MCPA, the concentrations used were 0.5, 1.0, 2.0, 4.0, and 8.0 mg/L, while for carbendazim and simazine, the concentrations were 0.25, 0.5, 1.0, 2.0, and 4.0 mg/L. The pH was not regulated. In the experiment on adsorption as a function of the initial pH value of pesticide solutions, 20 mg of each unmodified and modified adsorbent was placed in test tubes, and 5 ml of pesticide solutions with a concentration of 4 mg/L was added at pH 3, 5, 7, and 9. The pH value was regulated using 0.1 M HNO₃ and 0.1 M NaOH. Competitive adsorption of pesticides MCPA, carbendazim and simazine was tested for all adsorbents. 20 mg of each adsorbent was placed in test tubes, and 5 ml of pesticide solutions with a total concentration of 3 mg/L of MCPA, 3 mg/L of carbendazim, and 3 mg/L of simazine was added. The initial pH was not regulated and was equal to 4.9. For the kinetics of the adsorption experiment, 500 mg of selected adsorbent was placed in beakers, and 125 ml of pesticide solutions with a concentration of 4 mg/L was added. The initial pH was not regulated and was equal to 4.7 for 2,4-D, 4.8 for MCPA, 5.8 for carbendazim, and 5.8 for simazine. Samples were collected after 30 s, 1, 2, 5, 10, and 30 min, 1, 3, 5, 10, and 24 h to analyze the kinetics of adsorption.

All experiments were conducted under static conditions and at room temperature (25 °C). In the experiments examining adsorption concerning initial concentration, initial pH, and competitive adsorption, the samples underwent 24 h of stirring. Subsequently, they were subjected to centrifugation for a duration of 3 min at 14,000 rpm. The pesticide adsorption level was determined by comparing the initial and equilibrium concentrations. The stock solutions of pesticides were prepared by dissolving specific amounts of pesticide reagents in distilled water with the addition of 1% ethanol to enhance the solubility of pesticides.

Table 1
Properties of pesticides.

	2,4-D	MCPA	Simazine	Carbendazim
IUPAC name	2-(2,4-dichlorophenoxy)acetic acid	2-(4-chloro-2-methylphenoxy)acetic acid	6-chloro-2-N,4-N-diethyl-1,3,5-triazine-2,4-diamine	methyl N-(1H-benzimidazol-2-yl)carbamate
Structural Formula				
Chemical formula	C ₈ H ₆ Cl ₂ O ₃	C ₉ H ₉ ClO ₃	C ₇ H ₁₂ ClN ₅	C ₉ H ₉ N ₃ O ₂
Type	herbicide	herbicide	herbicide	fungicide
Molar mass [g/mol]	221.04	200.62	201.66	191.19
Solubility in water [mg/L] (25°C) ^a	311	294	6	8
pK _a ^b	2.81	2.93	0.11; 14.75	4.28; 9.70; 13.95
Molecule size [Å] ^c	5.60 × 10.09	5.86 × 10.09	4.48 × 11.47	5.04 × 10.73

^a Data obtained from safety data sheets of specific products.

^b Data calculated using Marvin 23.4.

^c Data calculated using VEGA ZZ v. 3.2.1.

2.3. Regeneration and cycles of adsorption

Chemical and thermal regeneration were performed to evaluate the potential for adsorbent reuse. For chemical regeneration, ethanol was used. 50 mg of selected adsorbents with adsorbed pesticides were taken in test tubes, and 5 ml of ethanol was added. The samples were stirred continuously for a period of 24 h, after which they underwent centrifugation lasting 3 min at a speed of 14,000 rpm. The regeneration effectiveness was determined by comparing the amount of pesticide adsorbed on the adsorbents and the amount of the pesticides washed out from adsorbents. Regenerated adsorbents were then used for repeated adsorption experiments. The cycles of adsorption-regeneration were performed four times.

Thermal regeneration was performed at different temperatures depending on the type of adsorbent and the pesticide adsorbed. X-FA-H and X-C-H with adsorbed 2,4-D and MCPA were heated at 200 °C, while X-FA and X-C with adsorbed carbendazim and simazine were heated at 350 °C. The selected temperatures were based on the decomposition temperatures of each pesticide and surfactant used for modification. The decomposition temperatures of carbendazim and simazine are around 300 [52] and 225 °C [53], respectively, while 2,4-D and MCPA decompose at temperatures around 140 [54] and 115 °C [55], respectively. HDTMA present on the surface of X-FA-H and X-C-H starts to decompose around 250 °C [49]. Therefore, X-FA-H and X-C-H with adsorbed 2,4-D and MCPA were heated at 200 °C, while X-FA and X-C with adsorbed carbendazim and simazine were heated at 350 °C. A sample of adsorbent with adsorbed pesticide was heated in the oven for 5 h, and then the adsorption of each pesticide was repeated. The adsorption-regeneration cycle was performed four times.

2.4. Analytical methods

The surface charge densities (σ_0) and points of zero charge (pH_{pzc}) of the adsorbents were determined using the potentiometric titration method at 22 °C in the pH range of 5.2–10, using an Eco Titrator (Metrohm, Herisau, Switzerland). The examined systems were titrated with 0.1 M NaOH in the pH range of 5.2–10. Initially, 50 ml of the supporting electrolyte (0.001 M and 0.01 NaCl) was titrated, followed by examining systems containing 100 mg of each adsorbent.

Transmission electron microscopy (TEM) observations were carried out on a Tecnai TF20 X-TWIN (FEG) microscope (FEI), working at an accelerating voltage of 200 kV. Samples for TEM observations were prepared by drop casting (powders suspended in water) on carbon coated copper TEM grids.

X-ray photoelectron spectroscopy (XPS) analyses were conducted on a PHI VersaProbeII Scanning XPS system using monochromatic Al K α (1486.6 eV) X-rays focused to a 100 μm spot and scanned over an area of 400 μm \times 400 μm . The photoelectron take-off angle was 45° and the pass energy in the analyzer was set to 117.50 eV (0.5 eV step) for survey scans and 46.95 eV (0.1 eV step) to obtain high energy resolution spectra for the C 1s, O 1s, Si 2p, Al 2p, Na 1s, Mg 2s, Fe 2p, K 2p and Ca 2p. Dual-beam charge compensation with 7 eV Ar⁺ ions and 1 eV electrons were used to maintain a constant sample surface potential regardless of sample conductivity. All XPS spectra were charge referenced to the unfunctionalized, saturated carbon (C–C) C 1s peak at 285.0 eV. The operating pressure in the analytical chamber was less than 3×10^{-9} mbar. Deconvolution of spectra was conducted using PHI MultiPak software (v.9.9.3). Spectrum background was subtracted using the Shirley method.

The amount of pesticides adsorbed onto the samples was measured using a Knauer high-performance liquid chromatography system equipped with a K-2600 UV detector and a 150 \times 4.6 mm, 5 μm , Knauer C18 column (Knauer, Berlin, Germany). Table 2 presents the conditions of the analytical method in detail. Thermogravimetric analysis/differential thermal analysis (TG/DTA) coupled with the analysis of the composition of evolved gases was performed using a Netzsch STA 449 F3 Jupiter apparatus (Netzsch, Chennai, India). For this purpose, the samples were heated at 30–1000 °C at a rate of 10 °C/min. The analyses were conducted under combustion conditions and in a helium atmosphere. The calibration curves were prepared by analyzing the stock solutions of each respective pesticide in the concentration range from 0.001 to 5 mg/L for carbendazim and simazine and from 0.001 to 10 mg/L for 2,4-D and MCPA. The data were fitted to linear regression with an R² coefficient equal to 0.99.

Table 2
Parameters of the chromatographic method.

Experiments of adsorption as a function of initial concentration, initial pH value, and kinetics				
	2,4-D	MCPA	Simazine	Carbendazim
Column	150 \times 4.6 mm, 5 μm , Knauer C18 column			
Mobile phase	Acetonitrile:Water (80:20); pH not regulated			
Flow [ml min ⁻¹]	1.5	1.5	1	1
Wavenumber [nm]	229	229	220	286
Retention time [min]	3.36	2.3	3.38	2.62
Detection limit [mg/L]	0.088	0.087	0.041	0.048
Experiment of competitive adsorption				
	2,4-D	MCPA	Simazine	Carbendazim
Column	–	250 \times 4.6 mm, 5 μm , Agilent Eclipse Plus C18		
Mobile phase	–	Acetonitrile:Water (80:20); pH not regulated		
Flow [ml min ⁻¹]	–	0.8		
Wavenumber [nm]	–	229		

2.5. Kinetics and adsorption isotherms

In the context of isotherm models, transforming nonlinear equations into linear forms can introduce biases, such as the appearance of poor linearity despite having high linear regression coefficients. There may also be a tendency for the Freundlich model to fit better at low experimental concentrations, while the Langmuir model fits better at higher experimental concentrations [56]. To circumvent these issues, the use of nonlinear optimization represents a mathematically rigorous approach for determining the parameters of the adsorption model while retaining the original equation form. In this study, we employ the nonlinear versions of adsorption isotherms and kinetics models to mitigate these potential problems.

Experimentally obtained adsorption data were fitted to Langmuir (LM), Freundlich (FM), Langmuir- Freundlich (LFM), Halsey (HM), and Jovanovic models (JM) represented by the equations (1)–(5), respectively.

The Langmuir equation:

$$q_e = \frac{Q_0 K_L C_e}{1 + K_L C_e} \quad (1)$$

where q_e is the pesticide adsorption capacity at equilibrium (mg/g); C_e is the equilibrium concentration of pesticide (mg/L); K_L is Langmuir constant (L/g); and Q_0 is the maximum adsorption capacity (mg/g).

The Freundlich equation:

$$q_e = K_F C_e^{1/n} \quad (2)$$

where q_e is the pesticide adsorption capacity at equilibrium (mg/g); K_F is Freundlich constant that refer to the adsorption capacity at unit concentration; C_e is the equilibrium concentration of pesticide (mg/L); and $1/n$ is adsorption intensity of the solute on the adsorbent.

The Langmuir-Freundlich equation:

$$q_e = \frac{Q_0 (K_a C_e)^n}{(K_a C_e)^n + 1} \quad (3)$$

where q_e is the pesticide adsorption capacity at equilibrium (mg/g); Q_0 is the maximum adsorption capacity (mg/g); C_e is the equilibrium concentration of pesticide (mg/L); K_a is the affinity constant for adsorption (L/mg); and n is the index of heterogeneity.

The Halsey isotherm:

$$q_e = \exp\left(\frac{\ln K_H + \ln C_e}{n}\right) \quad (4)$$

where q_e is the pesticide adsorption capacity at equilibrium (mg/g); C_e is the equilibrium concentration of pesticide (mg/L); and K_H and n are the Halsey isotherm constant and exponent, respectively.

The Jovanovic isotherm:

$$q_e = Q_0 (1 - e^{-(K_J C_e)}) \quad (5)$$

where q_e is the pesticide adsorption capacity at equilibrium (mg/g); C_e is the equilibrium concentration of pesticide (mg/L); Q_0 is the maximum adsorption capacity (mg/g); and K_J is the Jovanovic isotherm constant.

Experimentally obtained adsorption data were fitted to the following kinetics models: pseudo first order model (PFO), pseudo second order model (PSO), and Elovich represented by the equations (6)–(8), respectively.

Pseudo first order model:

$$q_t = C_e (1 - e^{-k_1 t}) \quad (6)$$

where t is time (min); q_t is adsorption capacity at equilibrium and given time (mg/g); C_e is the equilibrium concentration of pesticide (mg/L); and k_1 is first-order kinetic model constant.

Pseudo second order model:

$$q_t = \frac{C_e^2 k_2 t}{1 + C_e k_2 t} \quad (7)$$

where t is time (min); q_t is adsorption capacity at equilibrium and given time (mg/g); C_e is the equilibrium concentration of pesticide (mg/L); and k_2 is second-order kinetic model constant.

Elovich model:

$$q_t = \frac{1}{b} \ln(\alpha \beta t + 1) \quad (8)$$

where t is time (min); q_t is adsorption capacity at equilibrium and given time (mg/g); and α and β are constants.

3. Results

3.1. Characterization of adsorbents surfaces

3.1.1. Point of zero charge and surface charge density

Potentiometric titration was used to determine the points of zero charge (pH_{pzc}) and surface charge densities of zeolite and zeolite-carbon composite in the presence and absence of cationic and nonionic surfactants on the adsorbent surfaces. pH_{pzc} represents the point where the net surface charge is equal to zero. At pH values below pH_{pzc} , the solid surface is dominated by positive groups, and the chloride ions (Cl^-) of the supporting electrolyte reside in the Stern layer. Conversely, at pH values higher than pH_{pzc} , negative groups are dominant, and sodium ions (Na^+) form sheaths around the particles [57]. The results indicate that the pH_{pzc} of fly-ash-based unmodified zeolite and zeolite-carbon composite is below 5.2 (Fig. 1). A precise determination of pH_{pzc} was not possible due to the instability of the adsorbents in lower pH conditions. However, this value is consistent with literature reports on the pH_{pzc} of synthetic zeolites, which typically have a pH_{pzc} below 5 [58–60]. Modification of adsorbents with surfactants did not increase the pH_{pzc} value above 5.2, except for the X-FA-H sample, where pH_{pzc} is 5.35. The addition of surfactants alters the surface charge density (σ_0). The addition of HDTMA and Triton to the zeolite and zeolite-carbon composite surfaces leads to a noticeable increase in negative solid surface charge values (Fig. 1). In X-FA-H and X-C-H samples, quaternary amine groups in the HDTMA chains directed to the adsorbent surface contribute to an increase in absolute values of negative surface charge. In the case of X-FA-T and X-C-T samples, one contributing factor could be the partially negative charges associated with the oxygen atoms within the oxyethylene units of the TX100 molecule [61].

3.1.2. TEM

Bright-field (BF) TEM micrographs revealed that samples X-FA (Fig. 2a–d) and X–C (Fig. 2e–h) are composed mainly of zeolite type X with impurities derived from fly ash. The usual morphology of a zeolite X crystal is that of an octahedron, consisting of eight equilateral triangles [49,62–65]. However, in the case of X-FA and X–C, these crystals do not display the precisely shaped, characteristic octahedral morphology. Instead, they tend to overgrow each other, resulting in irregular and nearly rounded forms. One characteristic feature of both samples is the presence of rounded forms consisting of fine zeolite crystals that are empty inside (Fig. 2b and f). Modification of the zeolite and zeolite-carbon composite did not cause significant changes that can be observed in TEM micrographs (Figs. S1 and S2). The main conclusion drawn during the TEM observations was that the modified samples were far less stable during the analysis. Thus, it may be assumed that at high magnifications, the electron beam is destroying the surfactant molecules present on the surface of the adsorbents, causing damage to the observed grains. The samples are highly inhomogeneous, and besides the zeolite crystals, all unmodified and modified samples exhibit the presence of aluminosilicate cenospheres (Fig. 2c and S1a), mullite crystals (Fig. 2h and S1b), ettringite crystals (Fig. S3b), and foil-like morphology of argillite crystals (Figs. S2b and h) [66–68]. Additionally, the zeolite-carbon composite possesses a high content of unburned carbon, which can probably be seen in Figs. S3f and g [69]. Both X-FA and X–C materials exhibit the presence of skeleton-like morphology forms, which consist mainly of Al, Fe, and Mg (Fig. S3c).

3.1.3. XPS

Figs. S3–S8 present XPS spectra of X-FA, X–C materials, and their modified analogs. The Al 2p and Si 2p bands relate to the zeolite framework and do not exhibit significant trends upon surfactant modification, as well as Fe 2p_{3/2}, Ca 2p, Mg 2s, Na 1s, and K 2p bands originating from other mineral phases. After functionalization with HDTMA and TX-100, the intensity of the C–C band (285 eV) increased for both materials. By comparing the surface atomic composition (Tables S1 and S2), it is evident that more HDTMA was

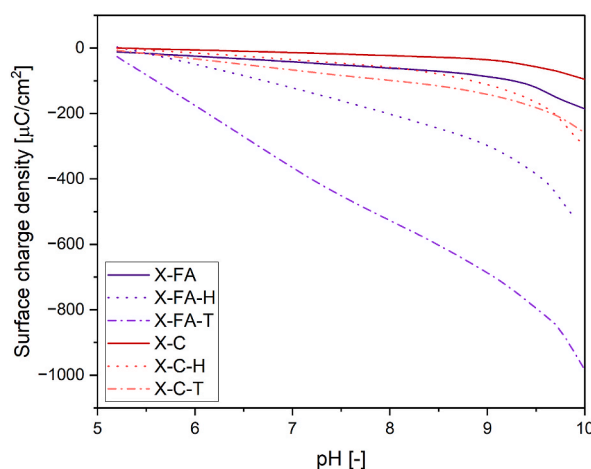


Fig. 1. Surface charge density of samples X-FA, X-FA-H, X-FA-T, X–C, X-C-H, and X-C-T.

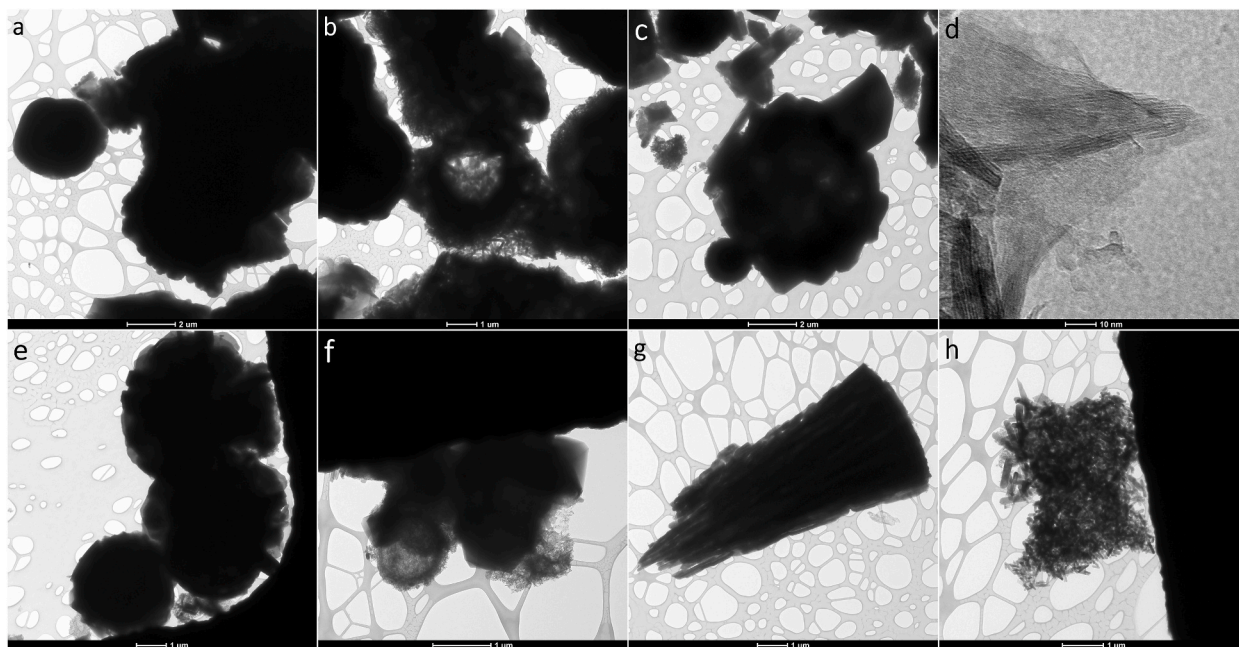


Fig. 2. BF TEM micrographs of sample X-FA (a–d) and sample X-C (e–h).

adsorbed on the surface of X-FA than TX-100. However, X-C adsorbed less HDTMA and more TX-100 than X-FA. Bands at 286.5 eV (C–O), 289.0 eV (O–C=O), and 532.2 eV (–OH) suggest the existence of functional groups containing oxygen of the carbonaceous matrix. Their intensity decreases upon surfactant coverage, with one exception. The X-C-T material shows a higher content of C–O bonds on the surface after modification. Meanwhile, C–N (400.1 eV), NH_4^+ (402.5), and Br^- (181.4 eV) bands appear only in the spectra of the X-C-H material.

3.2. Adsorption experiments

3.2.1. Adsorption as a function of initial pH value

The experiment examining the effect of the initial pH of the pesticide solution on adsorption revealed that the initial pH has a minimal influence on the removal of the chosen pesticides, and no distinct trends can be discerned. The analysis was carried out on unmodified samples of zeolite X-FA and zeolite-carbon composite X-C, samples modified with a cationic surfactant (X-FA-H and X-C-

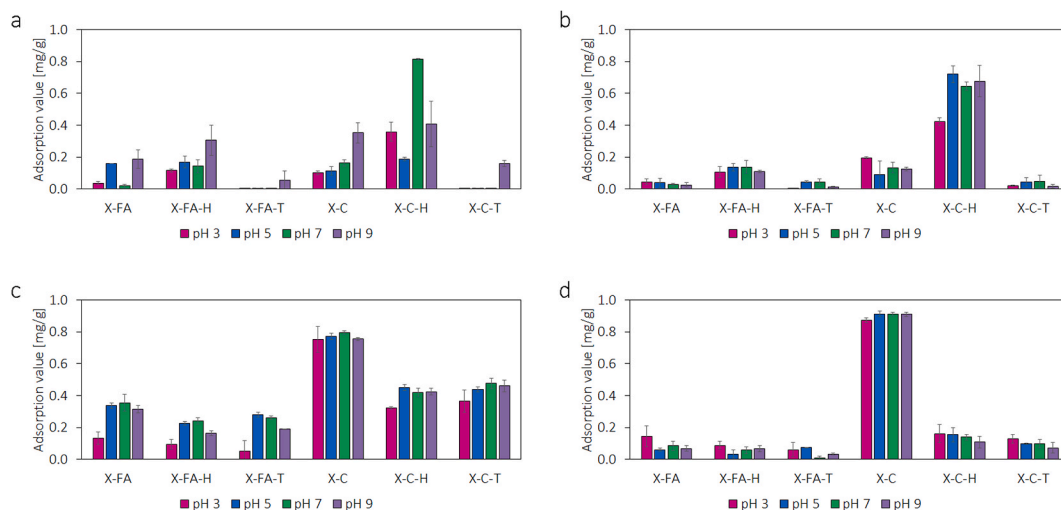


Fig. 3. Adsorption value of (a) 2,4-D, (b) MCPA, (c) carbendazim, and (d) simazine as a function of initial pH value on unmodified and modified adsorbents.

H), and samples modified with a nonionic surfactant (X-FA-T and X-C-T). Fig. S10 shows the equilibrium pH of the solutions after 24 h of adsorption. It is evident that the equilibrium pH is significantly higher than the initial pH of the solutions. For all zeolite samples and unmodified carbon-zeolite composites, the equilibrium pH ranges from 8 to 9.5 for initial pH 3 and 10 for initial pH 5, 7, and 9. The lower values are observed for samples X-C-H (6.8–8.6) and X-C-T (7.5–9.4).

Adsorbents with adsorbed 2,4-D and MCPA pesticides exhibit the widest differentiation in the results of adsorption at different initial pH values (Fig. 3a and b). For both pesticides, adsorption on HDTMA-modified samples is higher compared to unmodified zeolite and composite. The highest adsorption value was reached for HDTMA-modified zeolite-carbon composite, ranging from 0.187 to 0.813 mg/g for 2,4-D and 0.424–0.720 mg/g for MCPA. MCPA shows relatively low adsorption on samples modified with nonionic surfactant (X-FA-T and X-C-T), as well as unmodified zeolite for all initial pH conditions. 2,4-D also does not adsorb on samples modified with nonionic surfactant except for initial pH 9. At initial pH 9, adsorption is the highest for almost all groups of adsorbents. The adsorption capacity of carbendazim on the unmodified zeolite-carbon composite is the highest, reaching nearly 0.8 mg/g. In contrast, for the modified composites, it falls within the range of 0.366–0.474 mg/g, and for zeolites, it remains below 0.355 mg/g (Fig. 3c). Across all samples, a slight increase in adsorption is observed with variations in the initial pH; however, it appears that pH values of 5 and 7 are the most favorable for the adsorption of carbendazim.

The adsorption of simazine is also greater (around 0.9 mg/g) for unmodified zeolite-carbon composite, regardless of the pH, while modified zeolite-carbon composites exhibit significantly lower adsorption (less than 0.162 mg/g). Additionally, the higher the initial pH of the solution, the lower the removal of the pesticide (Fig. 3d). Adsorption on zeolite is ineffective, regardless of the modification, but in contrast to the composites, at low initial pH, adsorption seems to be slightly elevated.

3.2.2. Adsorption as a function of initial concentration

The outcomes of the experiment conducted to assess the impact of initial concentration on pesticide adsorption reveal that as the adsorbate's concentration in the solution rises, there is a corresponding increase in adsorption capacity (Fig. S11). This relationship holds true for all adsorbents, although it is particularly pronounced for carbendazim and simazine. The adsorption of these two pesticides is significantly greater when the initial concentration is set at 4 mg/L compared to other initial concentrations. 2,4-D and MCPA are also better adsorbed at higher concentrations (4 and 8 mg/L), but the increment is rather gradual and less predictable, especially for MCPA. Regrettably, none of the adsorbents reached their maximum adsorption capacity because the isotherm did not reach a plateau. Pesticides are known to have low solubility in water, so the feasibility of preparing a solution with a higher initial concentration was limited. Doing so would necessitate the use of an organic solvent, which is not applicable in environmental contexts.

To assess the potential adsorption capacity of the modified and unmodified zeolites and zeolite-carbon composites toward the investigated pesticides, the experimental data were fitted with Langmuir, Freundlich, Langmuir–Freundlich, Halsey, and Jovanovic models. The accuracy of the adsorption isotherms was estimated by the value of R^2 (Pearson correlation coefficient). Adsorption isotherms and their parameters are presented in Figs. S11–S12 and Table S3.

Considering the R^2 value as an indicator of proper fitting, it can be said that most experimental data obtained in this study fit more than one model. Usually, there is a slight difference in correlation coefficient R^2 , especially between Langmuir and Jovanovic models and between Freundlich and Halsey models. The differences between models are more evident at higher concentrations where the saturation point can be reached. However, at lower concentrations, the binding models may be virtually identical.

Samples of X-FA-based adsorbents with simazine exhibit the best fitting with the Freundlich isotherm, while X-C fits better with the Langmuir–Freundlich model and X-C-H and X-C-T fit the Langmuir, Freundlich, and Jovanovic models. Adsorbents with carbendazim fit mostly with the Freundlich and Halsey models, while adsorbents with 2,4-D may be described by the Langmuir–Freundlich model, except for X-FA, which fits better with the Freundlich and Halsey models and X-FA-H, which fits the Langmuir and Jovanovic models. The Freundlich model may also be attributed to the samples X-FA-H, X-FA-T, and X-C-T with adsorbed MCPA (Table S3).

According to Giles' classification system, adsorption isotherms can be assigned to one of the classes (S, L, H, and C) and then to one of the subgroups (1, 2, 3, 4, and mx) [70]. The assignment of Giles's isotherm class to the experimental isotherms obtained in this study is not straightforward, as the obtained isotherms exhibit diversity in the shapes of isotherms depending on the adsorbed pesticide and

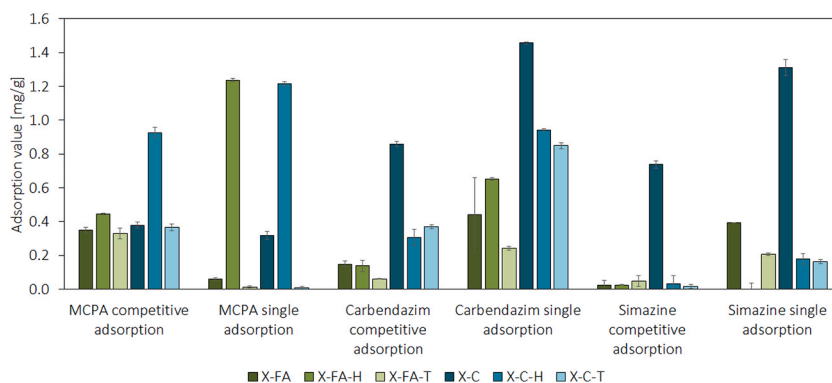


Fig. 4. Competitive adsorption of pesticides on unmodified and modified adsorbents.

the type of adsorbent and do not ideally fit into any of the four basic classes.

However, based on their initial slope, some assumptions can be made. Adsorption isotherms of the investigated pesticides mainly belong to the L-class, S-class, or S-class sloped to L-class with the subclass 1, 3, or mx (Figs. S11–S12). In most cases, the shape of the inflection was hard to define since the inflection occurred at low concentrations between the first two or three measurement points. The plateau was not reached for most samples, indicating that maximum adsorption was not achieved, especially for samples X-C-H with adsorbed 2,4-D, X-FA-H, and X-C with adsorbed carbendazim and simazine. Those samples exhibit a C1-class of isotherm in the analyzed range of pesticide concentration.

3.2.3. Competitive adsorption of pesticides

The results of the simultaneous adsorption of MCPA, carbendazim, and simazine are presented in Fig. 4. Competitive adsorption refers to the simultaneous adsorption of pesticides from the multi-component solution, while single adsorption refers to the adsorption from a solution containing only one pesticide. Adsorption of carbendazim and simazine from single-component solutions is higher than from multi-component solutions for all tested adsorbents. MCPA is most preferably adsorbed on zeolite and zeolite-carbon composite modified with a cationic surfactant, and for those materials, adsorption from a single-component solution is higher. The reverse trend can be observed for unmodified samples and samples modified with a nonionic surfactant. Especially, the adsorption efficiency on samples X-FA-T and X-C-T increases by more than 30% when carbendazim and simazine are present compared to the single adsorption of MCPA. Comparing the amount of each adsorbed pesticide from a multi-component solution revealed that all pesticides compete with each other for available active sites, and of all, simazine is the least preferably adsorbed. The exception is X-C adsorbent, which exhibits the highest adsorption capacity for both carbendazim and simazine, while all other adsorbents adsorb MCPA in the highest amounts. The equilibrium pH values of all samples were higher compared to the initial pH of the mixed pesticide solution. The increase from 7 to 9–10 was consistent with experiments of adsorption as a function of the initial pH value (Fig. S10).

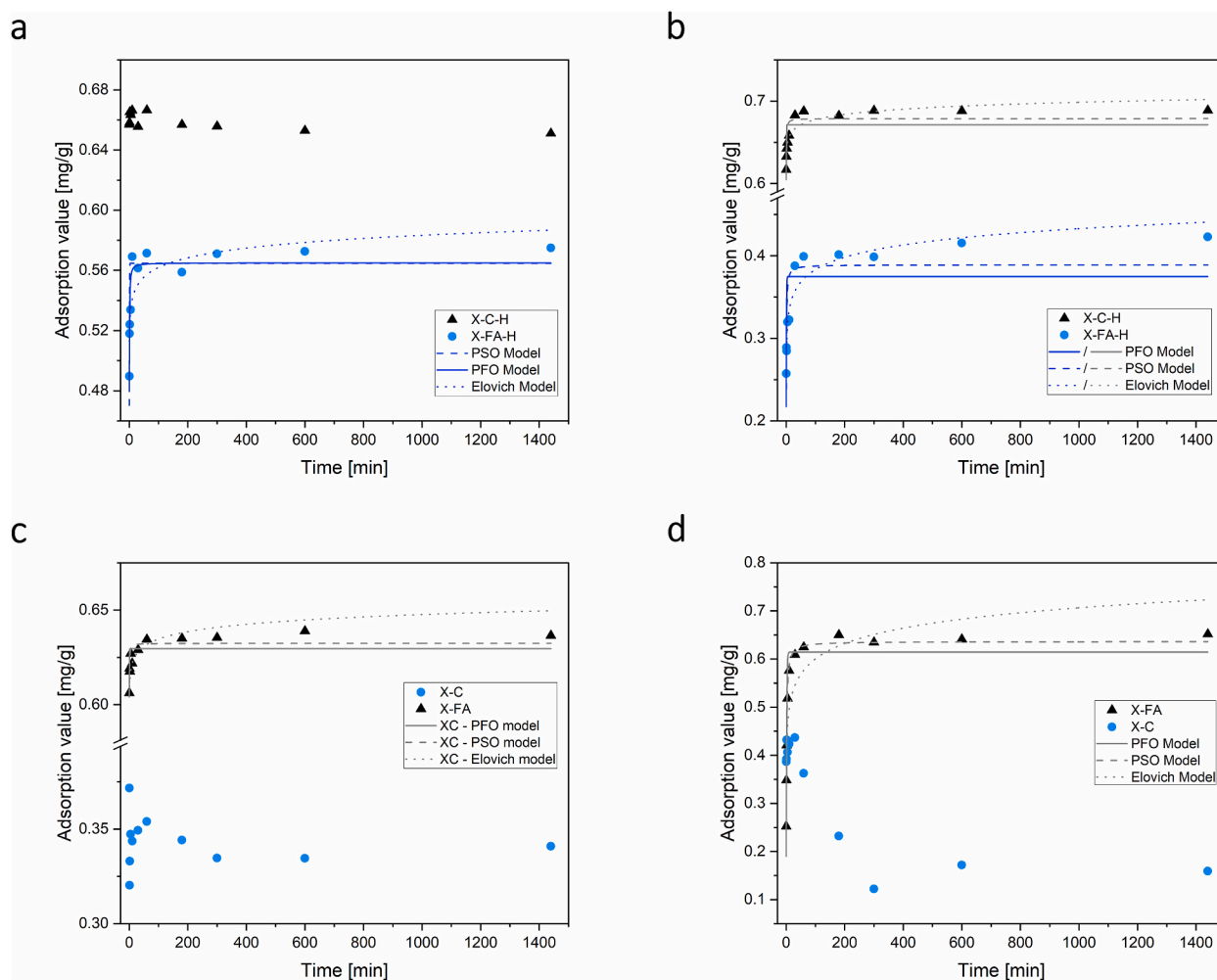


Fig. 5. Adsorption kinetics of (a) 2,4-D, (b) MCPA, (c) carbendazim, and (d) simazine.

3.2.4. Kinetics

Fig. 5 presents the plots for adsorption kinetics. The adsorption of all pesticides takes place rapidly, with equilibrium being attained within the initial few seconds of the experiment. Comparing modified and unmodified materials, X-C and X-C-H show higher adsorption capacity than X-FA and X-FA-H, respectively. However, the adsorption capacity of carbendazim (Fig. 5c) and simazine (Fig. 5d) on X-FA material decreases over time, resulting in abstract values for kinetic modeling. Therefore, we did not proceed with modeling for these samples. Similarly, the modeling of adsorption kinetics of 2,4-D (Fig. 5a) on X-C-H material gave abstract results, but the adsorption capacity is much higher and does not decrease rapidly. For MCPA (Fig. 5b), the results for both X-C-H and X-FA-H could be fitted to the kinetic models. The results of adsorption kinetics modeling are shown in Table S4. The adsorption isotherm of 2,4-D and MCPA on X-FA-H and X-C-H materials showed the highest R^2 for PSO and Elovich models. Meanwhile, the kinetics adsorption of simazine gave the best fitting for PFO and PSO models, and carbendazim for PSO and Elovich models.

3.3. Regeneration

Fig. 6 displays the results of regeneration experiments using an organic solvent. Four cycles were carried out, where each cycle involved the adsorption of pesticides on the surface of adsorbents and then removal with ethanol. Light-colored bars represent the amount of each pesticide adsorbed in each cycle of adsorption-regeneration, while dark-colored bars represent the amount of pesticide removed from the adsorbent. The results demonstrate that regeneration with ethanol and further reuse of adsorbents is possible.

X-C-H retains its adsorption capacity of 2,4-D and MCPA after each cycle of regeneration (Fig. 6a and b). In each cycle, X-C-H adsorbs almost 0.15 mg of 2,4-D or MCPA/1 g, and almost all the pesticide is removed during washing with ethanol. In contrast, adsorption on X-FA-H decreases almost two times after the first regeneration and then remains at a similar level for each further cycle. The amount of 2,4-D retained on X-FA-H and X-C-H after four cycles of adsorption-desorption was only 0.036 and 0.072 mg/g, respectively, while for MCPA, it was 0.093 mg/g for X-FA-H and 0.079 mg/g for X-C-H (Fig. S14). Regeneration of adsorbents with adsorbed carbendazim is the least effective (Fig. 6c). For both X-FA and X-C, the amount of carbendazim adsorbed is the highest in the first cycle of adsorption-desorption (0.075 and 0.143 mg/g, respectively), and then significantly decreases. Adsorption of simazine shows different trends, with X-FA exhibiting very low adsorption that increases after each regeneration process (Fig. 6d). Although the amount of simazine washed out during the regeneration of X-C is relatively low compared to the value of adsorption in the first cycle, the adsorption capacity of X-C in every further cycle is retained, which led to the retention of a significant amount of simazine on X-C (0.294 mg/g) (Fig. S14).

Fig. 7 displays the outcomes of thermal regeneration experiments conducted on the adsorbents using an organic solvent. Four cycles were carried out for each adsorbent, where pesticides were adsorbed on the surface of the adsorbents and then removed by heating at specified temperatures. For MCPA and 2,4-D, the regeneration temperature was selected to avoid the degradation of the HDTMA layer. Since the degradation temperatures of 2,4-D and MCPA are relatively low (115–140 °C) [54,55], and the HDTMA layer starts to decompose around 250 °C (with a maximum at 300 °C) [49], the temperature of 200 °C was chosen for regenerating X-FA-H and X-C-H adsorbents. On the other hand, simazine and carbendazim have higher degradation temperatures (227 and 300 °C,

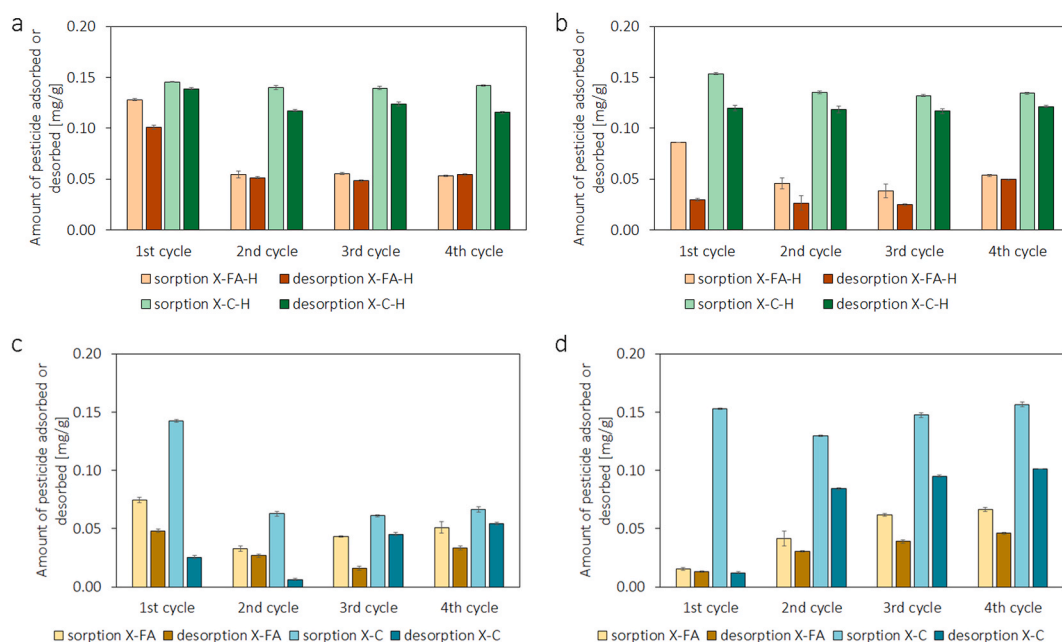


Fig. 6. Amount of (a) 2,4-D, (b) MCPA, (c) carbendazim, and (d) simazine adsorbed or desorbed during cycles of adsorption and regeneration using ethanol.

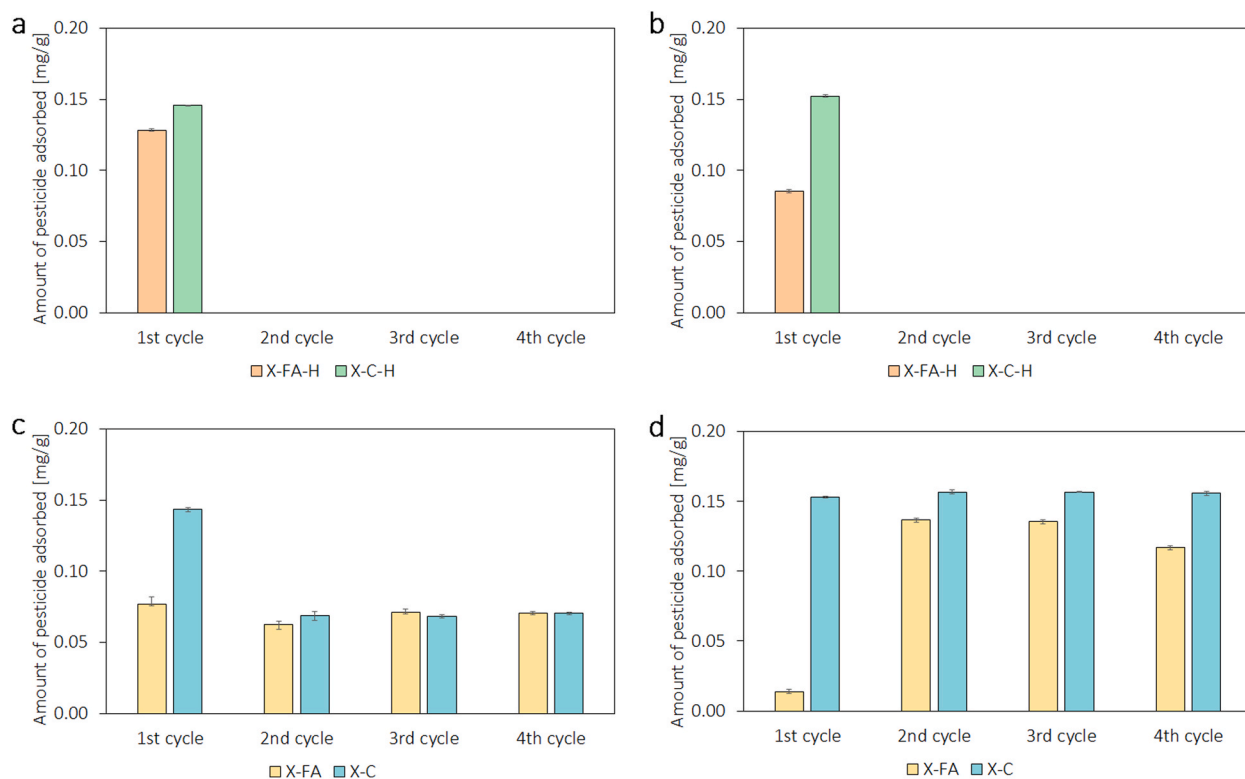


Fig. 7. Amount of (a) 2,4-D, (b) MCPA, (c) carbendazim, and (d) simazine adsorbed during cycles of adsorption and thermal regeneration.

respectively) and hence, the temperature of 350 °C was chosen for regenerating X-FA and X-C.

The effectiveness of regeneration depended on the type of pesticide. Adsorbents with adsorbed 2,4-D and MCPA could not be thermally regenerated (Fig. 7a and b). Heating at 200 °C did not remove the adsorbed pesticides or activate the surface, and therefore, 2,4-D or MCPA could not be adsorbed in further cycles. This indicates that the 2,4-D and MCPA adsorbed on X-FA-H and X-C-H were more stable and needed higher temperatures to begin decomposition than the pure 2,4-D and MCPA reagents. After the first heating, the adsorption of carbendazim on X-C decreased by two times, from 0.143 to 0.068 mg/g, which reached the same level as the adsorption on X-FA, which was consistent in each cycle of adsorption-regeneration (Fig. 7c). Adsorption of simazine on X-C in every further cycle was retained and reached more than 0.15 mg/g each time, and heating at 350 °C seemed to activate the surface of the X-FA adsorbent. Although the adsorption of simazine on X-FA in the first cycle was low (0.014 mg/g), it increased in subsequent cycles up to 0.117–0.137 mg/g (Fig. 7d).

The thermal decomposition of adsorbents before adsorption (Fig. 8 a-b) and with adsorbed pesticides (Fig. 8 c-f) were performed to assess the stability of adsorbents. The analysis of the gases released during heating allows for determining the temperature required for pesticide removal from the adsorbent. The slight DTA effects with a maximum of observed around 360–370 °C with the corresponding QMS-NO effects (m/z 30) indicate the decomposition of pesticides. The abundance of oxidized species released (e.g., NO) suggests that oxidative reactions facilitate the disintegration of the nitrogen-containing functional groups in carbendazim and simazine (such as the carbamate and benzimidazole group in carbendazim and the amine and triazine group in simazine). The oxidized species are present up to 900 °C for carbendazim (Fig. 8c and d) and 750 °C for simazine (Fig. 8e and f) until all residues of decomposition have been completely utilized by oxidative or combustion reactions related to the degradation of zeolite-carbon composite [71]. This study does not present the thermal decomposition of HDTMA-modified zeolite-carbon composite (X-C-H) with adsorbed 2,4-D and MCPA since the thermal regeneration of those adsorbents is not feasible. 2,4-D and MCPA decompose at low temperatures, which coincide with the decomposition temperatures of the surfactant. Furthermore, it's noteworthy that the quantity of adsorbed pesticides was relatively low, and no significant alterations were observed in the adsorbents before and after adsorption. All samples exhibited a substantial mass loss ranging from 46% to 50%. This mass loss can be attributed to several factors, including the release of structural and adsorbed water, the dissociation of calcite, oxidation of carbon, and degradation of the pesticides. The loss of water was confirmed by weak differential thermal analysis (DTA) effects occurring in the temperature range of 200–300 °C, along with corresponding mass spectrometry signals (QMS-CO effects, m/z 18). The DTA peak observed at approximately 600 °C may be attributed to the dissociation of calcite and the combustion of carbonaceous material, while the DTA peak around 900 °C could be related to structural breakdown and recrystallization processes [65]. Both dissociation, combustion, and structural breakdown led to the release of CO₂ that began around 500 °C.

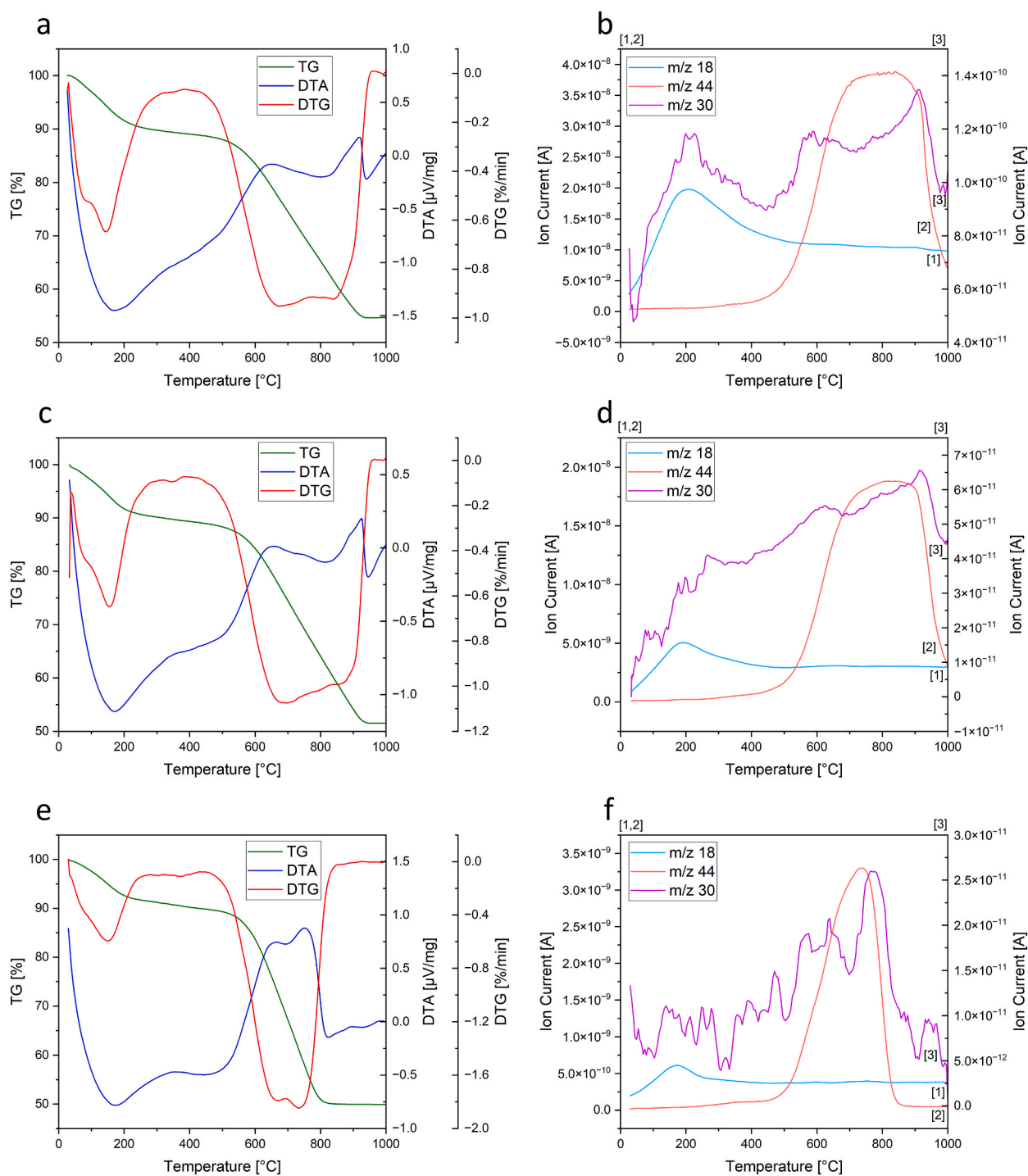


Fig. 8. TG/DTA in the air atmosphere of samples X-C (a and b), X-C with adsorbed carbendazim (c and d), and X-C with adsorbed simazine (e and f).

4. Discussion

The results obtained from the adsorption experiments using fly ash-based adsorbents suggest that the interactions between the active adsorbent surfaces and pesticides are complex. The study revealed that the influence of the initial pH of the pesticide solution on the removal of the selected pesticides was minimal, which contradicts data found in the literature. Typically, the efficiency of 2,4-D and MCPA adsorption on zeolitic materials usually is higher at low pH conditions, while for carbendazim and simazine, neutral or

slightly acidic pH values are preferred [72–76]. However, the composition of adsorbents synthesized from fly ash, which exhibit excellent pH-buffering properties, may explain the observed data. Regardless of the value of the initial pH of the pesticide solution, the equilibrium pH is always above 7.5 (Fig. S10) due to the alkaline character of the adsorbent surfaces resulting from the use of a high amount of NaOH in their synthesis. It should be noted that these zeolites and zeolite-carbon composites start to decompose if exposed to continuous contact with a solution pH of 5 or lower [49]. Thus, implementing a different approach where the pH of the pesticide solution is constantly controlled and corrected during the adsorption experiment would result in the dissolution of adsorbents. The results of potentiometric titration allowed for determining the pH_{pzc} of adsorbents. For most materials, a precise value of the pH_{pzc} could not be obtained since pH 5.2 was established as a dividing point below which adsorbents are unstable. However, the estimated values of pH_{pzc} indicate that at equilibrium pH obtained in experimental conditions (7.5–10), the surfaces of all adsorbents were negatively charged. Considering the pK_a of analyzed pesticides (Table 1), the pesticides exist in deprotonated forms of 2,4-D and MCPA, and the neutral form of simazine at equilibrium pH conditions (7.5–10), while for carbendazim, the neutral form is dominant at pH 7, and the contribution of the deprotonated form increases with increasing pH. Simazine and carbendazim are also more hydrophobic in comparison to highly polar 2,4-D and MCPA.

The XPS analysis of the surface chemical composition reveals the mechanisms of HDTMA and TX100 interactions with the zeolite and carbonaceous matrix. HDTMA is adsorbed on the surface of X-FA through ion exchange, with the hydrocarbon tail directed toward the solution and an ionic head attached to the surface of the zeolite [49]. This explains the observed increase in surface aliphatic carbon (Table 1 and Fig. S5). However, no HDTMA-derived nitrogen is detected, suggesting that the surfactant molecules are vertically oriented and may create a layer too thick for the analyzing beam to detect N atoms. Meanwhile, X-C material shows the presence of N atoms [49]. The C–N bonds on the surface of the unmodified material come from nitrogen atoms fixed in the carbonaceous matrix. However, after modification, nitrogen is mainly detected in the form of NH_4^+ (Table S2), as the nitrogen derived from HDTMA behaves similarly to the nitrogen derived from ammonium. The presence of nitrogen suggests that some of the HDTMA molecules are not vertically oriented with their hydrocarbon tails directed outward from the sample, as is the case in the X-FA-H sample. Instead, they lie in parallel or are directed with hydrocarbon tails to the surface carbonaceous matrix.

Adsorption of TX-100 on the X-C surface results in a significant increase of C–O bonds, indicating that TX-100 is attached to the surface of the carbonaceous matrix through the hydrophobic tail. In contrast, X-FA after TX-100 adsorption shows only a 1.5% increase in C–C bond abundance and no increase in C–O bond abundance (Table S1). Comparing these results with carbon content, which is 5.15 and 33.3%, respectively for X-FA and X-C one can conclude that nonionic surfactants do not react with the polar zeolite surface and are mainly adsorbed on the surface of the carbonaceous matrix. This explains why X-FA material retains only a small portion of TX-100.

The adsorption of 2,4-D and MCPA on unmodified zeolite and zeolite-carbon composite was ineffective due to electrostatic repulsion between negatively charged surfaces of adsorbents and negatively charged pesticide molecules. However, modification of the adsorbents with cationic surfactant enhanced the adsorption of 2,4-D and MCPA by introducing surfactant hydrocarbon tails that allowed the formation of hydrophobic bonds between adsorbent and adsorbate. Furthermore, the formation of a partial bilayer of HDTMA molecules was possible, particularly for X-C-H, where HDTMA molecules may lie parallel or be directed with hydrocarbon tails to the surface carbonaceous matrix [49]. Hydrophobic, electrostatic, and van der Waals interactions are also possible [77,78].

The quantity of surfactants utilized for modification corresponds to the ECEC of each material. While the aim is to attain an optimal surfactant monolayer on the adsorbent surface through the modification of zeolites and zeolite-carbon composites with 1 ECEC of HDTMA, there is a chance that partial bilayer formation and the precipitation of surfactant may occur [79–81]. This hypothesis was supported by estimating the amount of HDTMA washed from the surface of the modified adsorbents, revealing that using 1 ECEC of HDTMA does not result in the formation of an ideal surfactant monolayer [49]. A minor fraction, constituting up to 2% of HDTMA, might be loosely attached to the adsorbent and can be readily removed by water washing. Furthermore, the adsorption of surfactants is restricted to the external surface of the mineral due to the size of surfactant molecules, which prevents them from entering zeolite pores or reaching internal cation-exchange sites [81,82].

Carbendazim and simazine showed the most effective adsorption on the unmodified zeolite-carbon composite, and modification did not increase the adsorption capacity for either pesticide. For zeolite-carbon composites, where modifications significantly reduced the adsorption value, it can be assumed that active sites capable of binding to these pesticides are obstructed by the surfactant molecules, limiting adsorption. The highest adsorption was observed for zeolite-carbon composites, where carbonaceous matrix is covered with zeolite crystals, resulting in a material that exhibits characteristics of both zeolite and carbon. As a consequence, the composite contains not only the active sites typical of zeolite but also functional groups that originate from the carbon component. These functional groups may include carboxylic acid, lactone, carbonyl, and quinone groups, and they actively participate in the process of adsorption and immobilization of substances [49]. The primary mechanism accountable for the adsorption of carbendazim and simazine is likely the hydrophobic interaction occurring between the aromatic rings within the pesticide structures and the carbon present in zeolite-carbon composites. Partitioning may also contribute to the immobilization mechanisms involved [49,83,84].

The lack of significant changes in the adsorption values of carbendazim and simazine on zeolites modified with TX100 or HDTMA can be attributed to the fact that these pesticides do not compete with surfactants for active sites. It is possible that the layer of surfactant molecules on the surface of the zeolite provided new sites for the formation of hydrophobic interactions between the surfactant tails and the pesticide molecules, without blocking the active sites. Additionally, the higher adsorption values of carbendazim compared to simazine on unmodified and modified zeolites and modified zeolite-carbon composites may be due to the different speciation of the two pesticides at equilibrium pH conditions. In the pH range of 7.5–10, simazine exists only as a neutral molecule, whereas carbendazim exists mainly as a neutral molecule but can also exist in a deprotonated form as an anion. The presence of both speciations of carbendazim increases the adsorption due to the availability of active sites for both neutral and anionic molecules.

Results of competitive adsorption of carbendazim, simazine, and MCPA revealed that the adsorption of carbendazim and simazine from single-component solutions was higher compared to their adsorption from multi-component solutions for all tested adsorbents. This suggests that when both carbendazim and simazine are present together, they compete for the same active sites on the adsorbent surface, leading to a reduction in the adsorption capacity of these pesticides in the multi-component solution. The restricted availability of active sites on the adsorbent surface is the key factor behind this competitive effect. Furthermore, it was observed that the adsorption of carbendazim was higher than simazine, indicating that carbendazim is more preferentially adsorbed onto the adsorbent surface. Interestingly, the adsorption of MCPA from multi-component solutions was higher than from single-component solutions when unmodified adsorbents and TX-100-modified adsorbents were used. The presence of carbendazim and simazine on the adsorbent surface created an adsorption platform that generated attractive interaction forces, such as hydrogen bonding and p-p interactions, which enhanced MCPA adsorption. As a result, a synergistic effect was observed in the concurrent adsorption of MCPA, and this effect could be attributed to the formation of stacking layers of carbendazim and simazine on the zeolites and composites surface [32,85,86]. This phenomenon led to improved adsorption values for MCPA when it was present alongside carbendazim and simazine.

Giles' classification was used to classify the isotherms obtained in this study, and it was found that most of the isotherms can be attributed to the S or L-class, except for four cases (adsorption of 2,4-D on X-C-H, adsorption of MCPA on X-FA-H, adsorption of carbendazim on X-C, and adsorption of simazine on X-C), which exhibit features of C-class isotherms. C-class isotherms exhibit a constant adsorption affinity for a wide range of concentrations, and the availability of sites remains constant up to saturation [70,87]. At low concentrations, several organic substances behave similarly, particularly when the Langmuir equation serves as a proper model for the adsorption processes [87]. The isotherms that can be attributed to the C class describe the adsorption of pesticides on adsorbents that exhibit the highest adsorption value for specific pesticides. Among the adsorbents, X-C exhibits the most effective adsorption of carbendazim and simazine, and for this material, the C class isotherm is the most suitable. This finding suggests that, in applied experimental conditions, the availability of sites remains constant for the entire concentration range because the pesticide concentration was too low to saturate the adsorbent's surface active sites.

The shape of the initial slope that describes the change in availability of the adsorbents' active sites with increasing concentrations of pesticides can differentiate L and S class isotherms. For L-class isotherms, as more pesticide is adsorbed, the likelihood of remaining pesticide molecules finding a suitable site for adsorption decreases [70]. This behavior can be elucidated by the strong affinity of pesticides at low concentrations, which diminishes as the concentration rises. This is a result of the potent attractive forces between the adsorbate and adsorbent, contrasted with the weaker forces between the adsorbates themselves [88,89]. L class isotherms were applicable for the adsorption of MCPA on X-FA and X-C and simazine on X-FA-T, suggesting that the most effective adsorption of MCPA and simazine occurs at low concentrations, decreasing with increasing concentration, as shown in Figs. S12d and f, and l.

Conversely, S isotherms exhibit the opposite behavior, where the more molecules are already adsorbed, the easier it becomes for additional molecules to become immobilized. This suggests that adsorbed particles are associated side-by-side, which aids them in remaining attached to the surface, a phenomenon known as "cooperative adsorption" or "partitioning," usually observed for hydrophobic molecules [70]. The isotherms of adsorption of 2,4-D on X-FA-T and X-C-T, carbendazim on X-FA-H, X-C-H, and X-C-T, and simazine on X-FA, X-C-H, and X-C-T may be attributed to the S class. The hydrophobicity of simazine and carbendazim likely plays a significant role in their adsorption mechanisms. Furthermore, it should be noted that modification of zeolites and zeolite-carbon composites increases the adsorbents' surface hydrophobicity.

In some cases, the shape of the isotherm for certain pesticides and adsorbents was not clear, and mixed classes could be assigned, such as L-S or S-L. This was observed for 2,4-D adsorbed on X-FA and X-FA-H, MCPA adsorbed on X-FA-T, X-C-H, and X-C-T, carbendazim adsorbed on X-FA, and simazine adsorbed on X-FA-H. The alteration in the isotherm shape, transitioning from SS-type to L-type or vice versa, could be attributed to the steric hindrance imposed by the pesticide molecules. Proper orientation of the molecule is required to access the active site on the adsorbent surface. At low concentrations, the number of properly oriented molecules is low, while at higher concentrations, a higher number of molecules possess a favorable orientation, resulting in considerably higher adsorption. Thus, a change in the isotherm shape may be observed. This interpretation is supported by Sannino et al. [73], who observed a similar phenomenon during the adsorption of simazine onto H-Y zeolite.

When fitting our experimental data to popular isotherm models, we found that for most pesticides and adsorbents, there was only a slight difference in the correlation coefficient between the models. This phenomenon was primarily attributed to the low-concentration end of the isotherms. At low concentrations, the Jovanovic model essentially resembles Langmuir's model, as both models assume monolayer formation on the homogeneous surface of the adsorbent with no interactions among the adsorbed molecules. The primary distinction lies in the Jovanovic model's consideration of the surface binding vibrations of adsorbed molecules [90]. The assignment of the Jovanovic and Langmuir models to the adsorption of 2,4-D on X-FA-H and MCPA on X-C may indicate the homogeneity of the surface and the monolayer adsorption nature.

The Freundlich and Halsey isotherm models have similar assumptions, except for the theory of side-by-side interaction between adsorbed molecules, which is not considered in the Halsey model. According to the Halsey isotherm, interactions between molecules can be negligible since the heterogeneity of the surface influences the adsorption to a far greater extent. The Halsey isotherm is the most suitable for defining heteroporous solids and may be used to evaluate adsorption on a surface where active sites are situated at relatively large distances from each other [91,92]. The Freundlich and Halsey models can describe most of the analyzed adsorbents, including X-FA with adsorbed 2,4-D, carbendazim, and simazine, X-FA-H and X-FA-T with adsorbed MCPA, carbendazim, and simazine, X-C-H with adsorbed carbendazim, and X-C-T with adsorbed MCPA. Since both models assume heterogeneity of the adsorbent surface's active sites and multilayer or partial-multilayer adsorption, it can be assumed that at a selected range of concentration, the adsorption of 2,4-D, MCPA, carbendazim, and simazine on the mentioned adsorbents have features of multilayer adsorption on the heterogeneous surface.

The Langmuir–Freundlich isotherm model combines two theories: Langmuir's theory, which implies that adsorption occurs at distinct, energetically uniform adsorption sites, creating a complete monolayer, and Freundlich's theory, which maintains degree of non-uniform distribution of active sites while preventing an indefinite increase in the adsorbed amount with rising concentration. The main assumption of the Langmuir–Freundlich model is the heterogeneity of active sites. Therefore, experimental data that fit this model may indicate that pesticide adsorption occurs on active sites of different strengths [93–95]. The Langmuir–Freundlich isotherm model integrates elements of both Langmuir's and Freundlich's theories. Langmuir's theory posits that adsorption takes place at specific, energetically uniform sites, leading to the formation of a complete monolayer. Meanwhile, Freundlich's theory allows for a certain degree of heterogeneous distribution of active sites. However, the Langmuir–Freundlich model also prevents an unbounded increase in the adsorbed amount as the concentration rises. The Langmuir–Freundlich isotherm may be applied to the adsorption of 2,4-D on X-FA-T, X-C, and X-C-T, MCPA on X-C-H, carbendazim on X-C-T, and simazine on X-C, suggesting that adsorption occurs on active sites of different strengths.

Samples of X-C with adsorbed carbendazim, X-C-H with adsorbed 2,4-D and simazine, and X-C-T with adsorbed simazine can be fitted to a few isotherm models that are mutually exclusive and cannot be applied to the same sample. However, it should be noted that due to the low-concentration end of the isotherms, which was caused by experimental difficulties in solubilizing the pesticides in water, the maximum adsorption capacity was not reached in any sample. It is possible that providing experimental data of isotherms with high-concentration ends could result in a change in the shape of the isotherms, leading to a different best-fitted isotherm model. Therefore, the authors hesitate to unambiguously determine the nature of the adsorbent surfaces and adsorption parameters based solely on the isotherm models.

The effective regeneration and reuse of adsorbents are crucial from a practical standpoint. Regeneration with ethanol is the most effective for HDTMA-modified zeolite-carbon composites with adsorbed 2,4-D and MCPA. The amount of HDTMA used for modification was equal to 1.0 ECEC of each adsorbent, such that a monolayer should form, but in reality, a partial bilayer often occurs instead [49]. Washing the adsorbent with ethanol may remove the partial bilayer, leaving only the monolayer where the cationic part of the HDTMA molecule is directed toward the adsorbent surface and the hydrocarbon chain is directed outward. The reduction in adsorption capacity of X-FA-H toward 2,4-D and MCPA suggests that the presence of the partial bilayer was significantly responsible for enhanced adsorption, and that's why the adsorption of pesticides was lower in subsequent cycles of adsorption-regeneration in X-FA-H. However, for X-C-H, the adsorption capacity was preserved in each cycle, suggesting that the partial bilayer did not significantly contribute to the adsorption capacity, but rather electrostatic reactions and hydrophilic and hydrophobic interactions had a major impact on the adsorption of 2,4-D and MCPA on X-C-H [49].

The removal of these pesticides from the surface of adsorbents may be associated with interactions between the anionic forms of pesticides and the polar head of amphiphilic ethanol molecules through ion-dipole forces or the creation of hydrogen bonds between ethanol molecules and aromatic hydrogen atoms [78,96]. For carbendazim and simazine, the dominant mechanism of interaction may involve hydrophobic interactions between the aromatic rings in the structure of the pesticides and the carbon present in zeolite-carbon composites. Some research suggests that the application of ethanol enhances the hydrophobic interaction of hydrocarbon surfaces [97–99]. This may be the reason for the relatively high adsorption of carbendazim and simazine in cycles of adsorption-regeneration, despite the low regeneration efficiency.

In the case of thermal regeneration, it was observed that the chosen temperature of 350 °C for carbendazim and simazine was too low to achieve full pesticide decomposition, as shown by the evolution of nitric oxide (m/z 30) [49]. While the selected temperature did result in the release of structural and adsorbed water, it is unlikely that the adsorbents underwent significant transformations, as dissociation of calcite and combustion of the carbonaceous phase did not occur. Despite this, regeneration can still be considered successful for both X-FA and X-C with adsorbed carbendazim and simazine. However, regenerating HDTMA-modified zeolite-carbon composite with adsorbed 2,4-D and MCPA is more complicated. Although pure 2,4-D and MCPA can decompose at relatively low temperatures (120–140 °C) [54,55], heating at 200 °C does not seem to be sufficient for removing pesticides from the adsorbent surface. Additionally, using higher temperatures is not advised, as HDTMA begins to decompose around 250 °C [49], which would destroy the surfactant layer responsible for enhanced adsorption of 2,4-D and MCPA.

Table 3 presents a comparison of the adsorption capacities of different adsorbents toward 2,4-D, MCPA, carbendazim, and simazine. The aim of this comparison is to assess the potential of these adsorbents for pesticide adsorption. However, it is important to note that in some studies, the maximum adsorption capacity was not obtained, and the adsorption conditions and experimental design were significantly different, which can have a significant impact on the results. Moreover, in the present study, the concentrations of pesticides were chosen to be approximate to the concentrations found in potential real-life water samples, where pesticide concentrations are quite low. This may be the reason for the significant differences between adsorption capacities. Under unified experimental conditions, the adsorption capacities of the analyzed adsorbents may be less diverse. Although fly-ash-based zeolites and zeolite-carbon composites do not exhibit the highest adsorption capacity of pesticides compared to other adsorbents presented, they are worth considering as they are derived from the transformation of waste materials.

5. Conclusions

The study discovered that pesticide adsorption depended on the modification type used. Cationic surfactant increased MCPA and 2,4-D adsorption but reduced simazine and carbendazim, while nonionic surfactant slightly increased simazine adsorption. The low adsorption capacity may be due to pesticides' poor water solubility, preventing higher initial concentrations. pH had no significant impact on adsorption. Fly ash-based zeolites and zeolite-carbon composites had excellent buffering properties. Pesticide adsorption occurred rapidly, with most absorbed within 60 s. MCPA adsorption increased in the presence of other pesticides on unmodified and

Table 3
Comparison of adsorption values of adsorbents.

Pesticide	Adsorbent	Adsorption value [mg/g]	Reference
2,4-D	fly ash-based zeolite-carbon composite modified with HDTMA (X-C-H)	1.79	present study
	SBA-15-templated mesoporous carbon	136	[100]
	MCM-41 modified with 3-aminopropyltriethoxysilane	132	[101]
	HDTMA-modified zeolite Y in hydrogen form	35	[72]
	HDTMA-modified zeolite Y in sodium form	33	[72]
	activated carbon from wood composites	302.82	[102]
	HDTMA- modified montmorillonite	8.84	[103]
MCPA	fly ash-based zeolite-carbon composite modified with HDTMA (X-C-H)	1.62	present study
	agricultural waste materials (strawberry seeds and pistachio shells)	286.89–312.97	[104]
	DDTMA-modified montmorillonite	56.98	[105]
	activated carbon from wood composites	375.16	[102]
	goethite	10	[106]
Carbendazim	fly ash-based zeolite-carbon composite (X-C)	0.94	present study
	carbonized SBA-15	0.0098	[76]
	carbonized MCM-41	0.00829	[76]
	dealuminated NaY zeolite	0.00749	[76]
	zeolite MCM-22	0.01	[76]
	commercial bentonite	1.5	[107]
	activated carbon	32.31	[108]
Simazine	fly ash-based zeolite-carbon composite (X-C)	1.31	present study
	zeolite Y in hydrogen form	2.48	[73]
	activated carbon	28	[109]
	montmorillonite coated by hydroxy aluminum	0.25	[110]
	acid-activated beidellite	0.005	[111]
	porous silica	8.07	[112]

nonionic surfactant-modified samples. Moreover, regeneration was possible, but the method must be chosen based on the pesticide and adsorbent. Ethanol regenerated X-C-H with MCPA and 2,4-D, while thermal regeneration was not possible. Simazine and carbendazim adsorbents could be regenerated using both thermal and ethanol methods, with thermal regeneration of X-FA with simazine being more efficient. These results demonstrate the great potential of fly ash-based zeolites and zeolite-carbon composites for removing pesticides from water due to their rapid adsorption and effective regeneration without losing adsorption capacity. However, proper modification may be necessary to increase adsorption capacity for specific pesticides. Overall, these findings confirm the complex nature of interactions between zeolitic adsorbents and pesticides.

Authors' contributions

Magdalena Andrunik: Conceived and designed the experiments; Performed the experiments; Analyzed and interpreted the data; Wrote the paper. Mateusz Skalny: Performed the experiments; Analyzed and interpreted the data; Wrote the paper. Marta Gajewska, Mateusz Marzec: Performed the experiments; Analyzed and interpreted the data. Tomasz Bajda: Conceived and designed the experiments; Contributed reagents, materials, analysis tools or data; Wrote the paper.

Data availability statement

Data will be made available on request.

Funding source

The POIR.04.04.00-00-14E6/18-00. project is carried out within the TEAM-NET programme of the Foundation for Polish Science co-financed by the European Union under the European Regional Development Fund.

Declaration of competing interest

The authors declare that they have no known competing financial interests or personal relationships that could have appeared to influence the work reported in this paper.

Appendix A. Supplementary data

Supplementary data to this article can be found online at <https://doi.org/10.1016/j.heliyon.2023.e20572>.

References

- [1] G. Agoramorthy, Can India meet the increasing food demand by 2020? *Futures* 40 (2008) 503–506, <https://doi.org/10.1016/j.futures.2007.10.008>.
- [2] P.C. Abhilash, N. Singh, Pesticide use and application: an Indian scenario, *J. Hazard Mater.* 165 (2009) 1–12, <https://doi.org/10.1016/j.jhazmat.2008.10.061>.
- [3] T. Ahmad, M. Rafatullah, A. Ghazali, O. Sulaiman, R. Hashim, A. Ahmad, Removal of pesticides from water and wastewater by different adsorbents: a review, *J. Environ. Sci. Heal. Part C-Environmental Carcinog. Ecotoxicol. Rev.* 28 (2010) 231–271, <https://doi.org/10.1080/10590501.2010.525782>.
- [4] J. Wang, X.D. Liu, J. Lu, Urban River pollution control and remediation, *Procedia Environ. Sci.* 13 (2012) 1856–1862, <https://doi.org/10.1016/J.PROENV.2012.01.179>.
- [5] G.T. Miller, Biodiversity, in: *Sustain. Earth, sixth ed.*, Thompson Learning, Inc., Pacific Grove, CA, 1994, pp. 211–216.
- [6] M.R. Bonner, M.C.R. Alavanja, Pesticides, human health, and food security, *Food Energy Secur.* 6 (2017) 89–93, <https://doi.org/10.1002/fes3.112>.
- [7] R. Loos, B.M. Gawlik, G. Locoro, E. Rimaviciute, S. Contini, G. Bidoglio, EU-wide survey of polar organic persistent pollutants in European river waters, *Environ. Pollut.* 157 (2009) 561–568, <https://doi.org/10.1016/j.envpol.2008.09.020>.
- [8] V. Novotny, Diffuse pollution from agriculture - a worldwide outlook, *Water Sci. Technol.* 39 (1999) 1–13, [https://doi.org/10.1016/S0273-1223\(99\)00027-X](https://doi.org/10.1016/S0273-1223(99)00027-X).
- [9] R. Jayaraj, P. Megha, P. Sreedev, Organochlorine pesticides, their toxic effects on living organisms and their fate in the environment, *Interdiscipl. Toxicol.* 9 (2016) 90, <https://doi.org/10.1515/INTOX-2016-0012>.
- [10] J.L. Tadeo, Analysis of Pesticides in Food and Environmental Samples, second ed., CRC Press, Boca Raton, 2019 <https://doi.org/10.1201/9781351047081>.
- [11] J. Zacharia, Tano, identity, physical and chemical properties of pesticides, in: M. Stoytcheva (Ed.), *Pestic. Mod. World Trends Pestic. Anal.*, IntechOpen, Rijeka, Croatia, 2011, <https://doi.org/10.5772/17513>.
- [12] K.H. Buchel, Chemistry of pesticides, *J. Environ. Sci. Health Part B Pestic. Food Contam. Agric. Wastes B18* (1983) 419–643.
- [13] A. Marican, E.F. Durán-Lara, A review on pesticide removal through different processes, *Environ. Sci. Pollut. Res.* 25 (2018) 2051–2064, <https://doi.org/10.1007/s11356-017-0796-2>.
- [14] D.M. Hamby, Site remediation techniques supporting environmental restoration activities - a review, *Sci. Total Environ.* 191 (1996) 203–224, [https://doi.org/10.1016/S0048-9697\(96\)05264-3](https://doi.org/10.1016/S0048-9697(96)05264-3).
- [15] M. Cheng, G.M. Zeng, D.L. Huang, C. Lai, P. Xu, C. Zhang, Y. Liu, Hydroxyl radicals based advanced oxidation processes (AOPs) for remediation of soils contaminated with organic compounds: a review, *Chem. Eng. J.* 284 (2016) 582–598, <https://doi.org/10.1016/j.cej.2015.09.001>.
- [16] F.I. Khan, T. Husain, R. Hejazi, An overview and analysis of site remediation technologies, *J. Environ. Manag.* 71 (2004) 95–122, <https://doi.org/10.1016/j.jenvman.2004.02.003>.
- [17] S. Rani, D. Sud, Role of enhanced solar radiation for degradation of triazophos pesticide in soil matrix, *Sol. Energy* 120 (2015) 494–504, <https://doi.org/10.1016/j.solener.2015.07.050>.
- [18] A.O. Ibadon, P. Fitzpatrick, Heterogeneous photocatalysis: recent advances and applications, *Catalysts* 3 (2013) 189–218, <https://doi.org/10.3390/catal3010189>.
- [19] M.A. Matoug, Z.A. Al-Anber, T. Tagawa, S. Aljbour, M. Al-Shannag, Degradation of dissolved diazinon pesticide in water using the high frequency of ultrasound wave, *Ultrason. Sonochem.* 15 (2008) 869–874, <https://doi.org/10.1016/j.ultsonch.2007.10.012>.
- [20] S. Fukuzumi, Y.-M. Lee, J. Jung, W. Nam, Thermal and photocatalytic oxidation of organic substrates by dioxygen with water as an electron source, *Green Chem.* 20 (2018) 948–963, <https://doi.org/10.1039/c7gc03387g>.
- [21] K. Barbusinski, Fenton reaction - controversy concerning the chemistry, *Ecol. Chem. Eng. S-Chemia I Inz. Ekol. S.* 16 (2009) 347–358.
- [22] N.S. Ali, K.R. Kalash, A.N. Ahmed, T.M. Albayati, Performance of a solar photocatalysis reactor as pretreatment for wastewater via UV, UV/TiO₂, and UV/H₂O₂ to control membrane fouling, *Sci. Rep.* 12 (2022) 1–10, <https://doi.org/10.1038/s41598-022-20984-0>, 2022 121.
- [23] N.S. Abbood, N.S. Ali, E.H. Khader, H.S. Majdi, T.M. Albayati, N.M.C. Saady, Photocatalytic degradation of cefotaxime pharmaceutical compounds onto a modified nanocatalyst, *Res. Chem. Intermed.* 49 (2023) 43–56, <https://doi.org/10.1007/S11164-022-04879-3/METRICS>.
- [24] J. Zolgharnein, A. Shahmoradi, J. Ghasemi, Pesticides removal using conventional and low-cost adsorbents: a review, *Clean: Soil, Air, Water* 39 (2011) 1105–1119, <https://doi.org/10.1002/clen.201000306>.
- [25] F. Bonvin, L. Jost, L. Randin, E. Bonvin, T. Kohn, Super-fine powdered activated carbon (SPAC) for efficient removal of micropollutants from wastewater treatment plant effluent, *Water Res.* 90 (2016) 90–99, <https://doi.org/10.1016/j.watres.2015.12.001>.
- [26] M.S. Rodriguez-Cruz, M.J. Sanchez-Martin, M.S. Andrades, M. Sanchez-Camazano, Modification of clay barriers with a cationic surfactant to improve the retention of pesticides in soils, *J. Hazard Mater.* 139 (2007) 363–372, <https://doi.org/10.1016/j.jhazmat.2006.06.042>.
- [27] A. Legrouri, M. Lakraimi, A. Barroug, A. De Roy, J.P. Besse, Removal of the herbicide 2,4-dichlorophenoxyacetate from water to zinc-aluminium-chloride layered double hydroxides, *Water Res.* 39 (2005) 3441–3448, <https://doi.org/10.1016/j.watres.2005.03.036>.
- [28] G. Akcay, M. Akcay, K. Yurdakoc, The characterization of prepared organomontmorillonite (DEDAM) and sorption of phenoxyalkanoic acid herbicides from aqueous solution, *J. Colloid Interface Sci.* 296 (2006) 428–433, <https://doi.org/10.1016/j.jcis.2005.09.014>.
- [29] S.B. Wang, H.W. Wu, Environmental-benign utilisation of fly ash as low-cost adsorbents, *J. Hazard Mater.* 136 (2006) 482–501, <https://doi.org/10.1016/j.jhazmat.2006.01.067>.
- [30] S. Mohsen Alardhi, J.M. Alrubaye, T.M. Albayati, Removal of methyl green dye from simulated waste water using hollow fiber ultrafiltration membrane, *IOP Conf. Ser. Mater. Sci. Eng.* 928 (2020), 052020, <https://doi.org/10.1088/1757-899X/928/5/052020>.
- [31] H.J. Al-Jaaf, N.S. Ali, S.M. Alardhi, T.M. Albayati, Implementing eggplant peels as an efficient bio-adsorbent for treatment of oily domestic wastewater, *Desalination Water Treat.* 245 (2022) 226–237, <https://doi.org/10.5004/dwt.2022.27986>.
- [32] M. Ashrul Asbollah, M.S.M. Sahid, K.M. Padmosoedarso, A.H. Mahadi, E. Kusriani, J. Hobley, A. Usman, Individual and competitive adsorption of negatively charged acid blue 25 and acid red 1 onto raw Indonesian kaolin clay, *Arabian J. Sci. Eng.* 47 (2022), <https://doi.org/10.1007/s13369-021-06498-3>.
- [33] K. Rida, S. Bouraoui, S. Hadnine, Adsorption of methylene blue from aqueous solution by kaolin and zeolite, *Appl. Clay Sci.* (2013) 83–84, <https://doi.org/10.1016/j.clay.2013.08.015>.
- [34] D. Ziolkowska, A. Shyichuk, I. Karwasz, M. Witkowska, Adsorption of cationic and anionic dyes onto commercial kaolin, *Adsorpt. Sci. Technol.* 27 (2009), <https://doi.org/10.1260/026361709789625306>.
- [35] A. Bielecka, J. Kulczycka, Coal combustion products management toward a circular economy—a case study of the coal power plant sector in Poland, *Energies* 13 (2020) 3603, <https://doi.org/10.3390/EN13143603>, 13 (2020) 3603.
- [36] M.G. Miricioiu, V.C. Niculescu, Fly ash, from recycling to potential raw material for mesoporous silica synthesis, *Nanomaterials* 10 (2020), <https://doi.org/10.3390/nano10030474>.
- [37] C. Belviso, F. Cavalcante, F. Javier Huertas, A. Lettino, P. Ragone, S. Fiore, The crystallisation of zeolite (X- and A-type) from fly ash at 25 °C in artificial sea water, *Microporous Mesoporous Mater.* 162 (2012) 115–121, <https://doi.org/10.1016/j.micromeso.2012.06.028>.
- [38] D. Li, H. Min, X. Jiang, X. Ran, L. Zou, J. Fan, One-pot synthesis of Aluminium-containing ordered mesoporous silica MCM-41 using coal fly ash for phosphate adsorption, *J. Colloid Interface Sci.* 404 (2013) 42–48, <https://doi.org/10.1016/j.jcis.2013.04.018>.
- [39] C. Chen, J. Kim, W.S. Ahn, CO₂ capture by amine-functionalized nanoporous materials: a review, *Kor. J. Chem. Eng.* 31 (2014) 1919–1934, <https://doi.org/10.1007/s11814-014-0257-2>.
- [40] P.N. Diagbaya, B.I. Olu-Owolabi, K.O. Adebowale, Microscale scavenging of pentachlorophenol in water using amine and triphosphoate-grafted SBA-15 silica: batch and modeling studies, *J. Environ. Manag.* 146 (2014) 42–49, <https://doi.org/10.1016/j.jenvman.2014.04.038>.
- [41] Z. Wu, D. Zhao, Ordered mesoporous materials as adsorbents, *Chem. Commun.* 47 (2011) 3332–3338, <https://doi.org/10.1039/c0cc04909c>.
- [42] J. Mokrzycki, M. Fedyna, M. Marzec, J. Szerement, R. Panek, A. Klimek, T. Bajda, M. Mierzwa-Hersztel, Copper ion-exchanged zeolite X from fly ash as an efficient adsorbent of phosphate ions from aqueous solutions, *J. Environ. Chem. Eng.* 10 (2022), 108567, <https://doi.org/10.1016/J.JECE.2022.108567>.
- [43] P.T. Huong, B.K. Lee, J. Kim, C.H. Lee, Nitrophenols removal from aqueous medium using Fe-nano mesoporous zeolite, *Mater. Des.* 101 (2016) 210–217, <https://doi.org/10.1016/J.MATDES.2016.04.020>.

- [44] M.E. Davis, R.F. Lobo, Zeolite and molecular sieve synthesis, *Chem. Mater.* 4 (1992) 756–768, <https://doi.org/10.1021/cm00022a005>.
- [45] N.F. Gao, S. Kume, K. Watari, Zeolite-carbon composites prepared from industrial wastes: (I) Effects of processing parameters, *Mater. Sci. Eng. a-Structural Mater. Prop. Microstruct. Process.* 399 (2005) 216–221, <https://doi.org/10.1016/j.msea.2005.04.008>.
- [46] N.F. Gao, S. Kume, K. Watari, Zeolite-carbon composites prepared from industrial wastes: (II) evaluation of the adaptability as environmental materials, *Mater. Sci. Eng. a-Structural Mater. Prop. Microstruct. Process.* 404 (2005) 274–280, <https://doi.org/10.1016/j.msea.2005.05.090>.
- [47] H. Marsh, E.A. Heintz, F. Rodríguez-Reinos, Introduction to carbon, *Nanosci. Technol.* 5 (2013) 1–5, https://doi.org/10.1007/978-3-642-30490-3_1.
- [48] P. Arnnok, R. Burakkham, Retention of carbamate pesticides by different surfactant-modified sorbents: comparative study, *J. Braz. Chem. Soc.* 25 (2014) 1720–1729, <https://doi.org/10.5935/0103-5053.20140167>.
- [49] M. Andrunik, M. Skalny, T. Bajda, Functionalized adsorbents resulting from the transformation of fly ash: characterization, modification, and adsorption of pesticides, *Sep. Purif. Technol.* 309 (2023), 123106, <https://doi.org/10.1016/J.SEPPUR.2023.123106>.
- [50] M. Wdowin, M. Franus, R. Panek, L. Badura, W. Franus, The conversion technology of fly ash into zeolites, *Clean Technol. Environ. Policy* 16 (2014) 1217–1223, <https://doi.org/10.1007/s10098-014-0719-6>.
- [51] L. Bandura, R. Panek, J. Madej, W. Franus, Synthesis of zeolite-carbon composites using high-carbon fly ash and their adsorption abilities towards petroleum substances, *Fuel* 283 (2021), 119173, <https://doi.org/10.1016/j.fuel.2020.119173>.
- [52] Carbazepim | C9H9N3O2 - PubChem, (n.d.). <https://pubchem.ncbi.nlm.nih.gov/compound/Carbazepim> (accessed February 25, 2023)..
- [53] Simazine | C7H12ClN5 - PubChem, (n.d.). <https://pubchem.ncbi.nlm.nih.gov/compound/Simazine> (accessed February 25, 2023)..
- [54] 2,4-Dichlorophenoxyacetic acid | C8H6Cl2O3 - PubChem, (n.d.). https://pubchem.ncbi.nlm.nih.gov/compound/2_4-Dichlorophenoxyacetic-acid (accessed February 25, 2023)..
- [55] 4-Chloro-2-methylphenoxy)acetic acid | C9H9ClO3 - PubChem (n.d.). https://pubchem.ncbi.nlm.nih.gov/compound/4-Chloro-2-methylphenoxy_acetic-acid (accessed February 25, 2023)..
- [56] H.N. Tran, S.J. You, A. Hosseini-Bandegharai, H.P. Chao, Mistakes and inconsistencies regarding adsorption of contaminants from aqueous solutions: a critical review, *Water Res.* 120 (2017) 88–116, <https://doi.org/10.1016/j.watres.2017.04.014>.
- [57] K. Szewczuk-Karpisz, P. Krasucka, P. Boguta, K. Skic, Z. Sokotowska, G. Fijałkowska, M. Wiśniewska, Electrical double layer at the gibbsite/anionic polyacrylamide/supporting electrolyte interface – adsorption, spectroscopy and electrokinetic studies, *J. Mol. Liq.* 261 (2018) 439–445, <https://doi.org/10.1016/J.MOLLIQ.2018.04.030>.
- [58] M. Kosmulski, pH-dependent surface charging and points of zero charge. IV. Update and new approach, *J. Colloid Interface Sci.* 337 (2009) 439–448, <https://doi.org/10.1016/J.JCIS.2009.04.072>.
- [59] M. Kosmulski, The pH dependent surface charging and points of zero charge. VII. Update, *Adv. Colloid Interface Sci.* 251 (2018) 115–138, <https://doi.org/10.1016/J.CIS.2017.10.005>.
- [60] M. Kosmulski, The pH dependent surface charging and points of zero charge. VIII. Update, *Adv. Colloid Interface Sci.* 275 (2020), 102064, <https://doi.org/10.1016/J.CIS.2019.102064>.
- [61] X. Zeng, K. Osseo-Asare, Partitioning behavior of silica in the Triton X-100/dextran/water aqueous biphasic system, *J. Colloid Interface Sci.* 272 (2004) 298–307, <https://doi.org/10.1016/J.JCIS.2003.11.009>.
- [62] H.J. Lee, Y.M. Kim, O.S. Kweon, I.J. Kim, Structural and morphological transformation of NaX zeolite crystals at high temperature, *J. Eur. Ceram. Soc.* 27 (2007) 561–564, <https://doi.org/10.1016/j.jeurceramsoc.2006.04.156>.
- [63] H.J. Lee, Y.M. Kim, O.S. Kweon, I.J. Kim, Crystal growing and reaction kinetic of large NaX zeolite crystals, *J. Eur. Ceram. Soc.* 27 (2007) 581–584, <https://doi.org/10.1016/j.jeurceramsoc.2006.04.112>.
- [64] O. Dere Ozdemir, S. Piskin, A novel synthesis method of zeolite X from coal fly ash: alkaline fusion followed by ultrasonic-assisted synthesis method, *Waste and Biomass Valorization* 10 (2019) 143–154, <https://doi.org/10.1007/s12649-017-0050-7>.
- [65] D.W. Breck, *Zeolite Molecular Sieves - Structure, Chemistry, and Use*, John Wiley & Sons, 1974. <https://app.knovel.com/web/toc.v/cid:kpZMSSCU04/viewerType:toc/>. (Accessed 16 November 2020).
- [66] I. Techer, D. Bartier, P. Boulvais, E. Tinsau, K. Suchorski, J. Cabrera, A. Dauzères, Tracing interactions between natural argillites and hyper-alkaline fluids from engineered cement paste and concrete: chemical and isotopic monitoring of a 15-years old deep-disposal analogue, *Appl. Geochem.* 27 (2012) 1384–1402, <https://doi.org/10.1016/J.APGEOCHEM.2011.08.013>.
- [67] C. Khatri, D. Jain, A. Rani, Fly ash-supported cerium triflate as an active recyclable solid acid catalyst for Friedel-Crafts acylation reaction, *Fuel* 89 (2010) 3853–3859, <https://doi.org/10.1016/J.FUEL.2010.07.007>.
- [68] M. Romero, I. Padilla, M. Contreras, A. López-delgado, Mullite-based ceramics from mining waste: a review, *Minerals* 11 (2021), <https://doi.org/10.3390/MIN11030332>.
- [69] P. Sielicki, H. Janik, A. Guzman, J. Namieśnik, Grain type and size of particulate matter from diesel vehicle exhausts analysed by transmission electron microscopy, *Environ. Technol.* 33 (2012) 1781–1788, <https://doi.org/10.1080/09593330.2011.646315>.
- [70] C.H. Giles, D. Smith, A. Huitson, A general treatment and classification of the solute adsorption isotherm. I. Theoretical, *J. Colloid Interface Sci.* 47 (1974) 755–765, [https://doi.org/10.1016/0021-9797\(74\)90252-5](https://doi.org/10.1016/0021-9797(74)90252-5).
- [71] O. Senneca, F. Scherillo, A. Nunziata, Thermal degradation of pesticides under oxidative conditions, *J. Anal. Appl. Pyrolysis* 80 (2007) 61–76, <https://doi.org/10.1016/J.JAAP.2007.01.002>.
- [72] Y. Pukcothanung, T. Siritanon, K. Rangsiwatananon, The efficiency of zeolite Y and surfactant-modified zeolite Y for removal of 2,4-dichlorophenoxyacetic acid and 1,1'-dimethyl-4,4'-bipyridinium ion, *Microporous Mesoporous Mater.* 258 (2018) 131–140, <https://doi.org/10.1016/j.micromeso.2017.08.035>.
- [73] F. Sannino, S. Ruocco, A. Marocco, S. Esposito, M. Pansini, Cyclic process of simazine removal from waters by adsorption on zeolite H-Y and its regeneration by thermal treatment, *J. Hazard Mater.* 229–230 (2012) 354–360, <https://doi.org/10.1016/J.JHAZMAT.2012.06.011>.
- [74] F. Sannino, A. Marocco, E. Garrone, S. Esposito, M. Pansini, Adsorption of simazine on zeolite H-Y and sol-gel technique manufactured porous silica: a comparative study in model and natural waters, *J. Environ. Sci. Health Part B Pestic. Food Contam. Agric. Wastes* 50 (2015) 777–787, <https://doi.org/10.1080/03601234.2015.1058094>.
- [75] S. Esposito, E. Garrone, A. Marocco, M. Pansini, P. Martinelli, F. Sannino, Application of highly porous materials for simazine removal from aqueous solutions, *Environ. Technol.* 37 (2016) 2428–2434, <https://doi.org/10.1080/09593330.2016.1151461>.
- [76] J.L. Chen, L. Gao, Q. Jiang, Q. Hou, Y. Hong, W. Jian Shen, Y. Wang, J.H. Zhu, Fabricating efficient porous sorbents to capture organophosphorus pesticide in solution, *Microporous Mesoporous Mater.* 294 (2020), <https://doi.org/10.1016/j.micromeso.2019.109911>.
- [77] M. Shirvani, E. Farajollahi, S. Bakhtiari, O.A. Ogunseitan, Mobility and efficacy of 2,4-D herbicide from slow-release delivery systems based on organo-zeolite and organo-bentonite complexes, 255–262, <https://doi.org/10.1080/03601234.2014.868275>, 2014.
- [78] S. Bakhtiari, M. Shirvani, H. Shariatmadari, Adsorption-desorption behavior of 2,4-D on NCP-modified bentonite and zeolite: implications for slow-release herbicide formulations, *Chemosphere* 90 (2013) 699–705, <https://doi.org/10.1016/J.CHEMOSPHERE.2012.09.052>.
- [79] R. Hojiyev, G. Ersever, I.E. Karağaçoğlu, F. Karakaş, F. Boylu, Changes on montmorillonite characteristics through modification, *Appl. Clay Sci.* (2016) 127–128, <https://doi.org/10.1016/J.CLAY.2016.03.042>, 105–110.
- [80] A. Solińska, T. Bajda, Modified zeolite as a sorbent for removal of contaminants from wet flue gas desulphurization wastewater, *Chemosphere* (2022) 286, <https://doi.org/10.1016/J.CHEMOSPHERE.2021.131772>.
- [81] Z. Li, R.S. Bowman, Counterion effects on the sorption of cationic surfactant and chromate on natural clinoptilolite, *Environ. Sci. Technol.* 31 (1997) 2407–2412, <https://doi.org/10.1021/ES9610693>.
- [82] G.M. Haggerty, R.S. Bowman, Sorption of chromate and other inorganic anions by organo-zeolite, *Environ. Sci. Technol.* 28 (1994) 452–458, <https://doi.org/10.1021/es00052a017>.
- [83] T. Wang, Z. Zhang, H. Zhang, X. Zhong, Y. Liu, S. Liao, X. Yue, G. Zhou, Sorption of carbendazim on activated carbons derived from rape straw and its mechanism, *RSC Adv.* 9 (2019) 41745–41754, <https://doi.org/10.1039/C9RA06495H>.

- [84] G.L. Kyriakopoulos, D. Doulia, Adsorption of pesticides on carbonaceous and polymeric materials from aqueous solutions: a review, *Separ. Purif. Rev.* 35 (2006) 97–191, <https://doi.org/10.1080/15422110600822733>.
- [85] M.A. Asbollah, A.H. Mahadi, E. Kusriani, A. Usman, Synergistic effect in concurrent removal of toxic methylene blue and acid red-1 dyes from aqueous solution by durian rind: kinetics, isotherm, thermodynamics, and mechanism, *Int. J. Phytoremediation* 23 (2021), <https://doi.org/10.1080/15226514.2021.1901851>.
- [86] M.A. Asbollah, M.S.M. Sahid, E.W.E.S. Shahrin, N.A.H. Narudin, E. Kusriani, N.N.M. Shahri, J. Hobley, A. Usman, Dynamics and thermodynamics for competitive adsorptive removal of methylene blue and rhodamine B from binary aqueous solution onto durian rind, *Environ. Monit. Assess.* 194 (2022), <https://doi.org/10.1007/s10661-022-10332-0>.
- [87] C. Hinze, Description of sorption data with isotherm equations, *Geoderma* 99 (2001) 225–243, [https://doi.org/10.1016/S0016-7061\(00\)00071-9](https://doi.org/10.1016/S0016-7061(00)00071-9).
- [88] P. Sips, Searching for optimum adsorption curve for metal sorption on soils: comparison of various isotherm models fitted by different error functions, *SN Appl. Sci.* 3 (2021) 1–13, <https://doi.org/10.1007/s42452-021-04383-0/FIGURES/3>.
- [89] D.L. Sparks, Sorption phenomena on soils, in: *Environ. Soil Chem.*, Elsevier, 2003, pp. 133–186, <https://doi.org/10.1016/B978-012656446-4/50005-0>.
- [90] D.S. Jovanović, Physical adsorption of gases - I: isotherms for monolayer and multilayer adsorption, *Kolloid-Z. Z. Polym.* 235 (1969) 1203–1213, <https://doi.org/10.1007/BF01542530/METRICS>.
- [91] G. Halsey, Physical adsorption on non-uniform surfaces, *J. Chem. Phys.* 16 (1948) 931, <https://doi.org/10.1063/1.1746689>.
- [92] N. Ayawei, A.N. Ebelegi, D. Wankasi, Modelling and interpretation of adsorption isotherms, *J. Chem.* 2017 (2017), <https://doi.org/10.1155/2017/3039817>.
- [93] A. Jevremovic, P. Bober, M. Micusik, J. Kulicek, U. Acharya, J. Pfeleger, M. Milojevic-Rakic, D. Krajsnik, M. Trchova, J. Stejskal, G. Ciric-Marjanovic, Synthesis and characterization of polyaniline/BEA zeolite composites and their application in nicosulfuron adsorption, *Microporous Mesoporous Mater.* 287 (2019) 234–245, <https://doi.org/10.1016/j.micromeso.2019.06.006>.
- [94] D. Bajuk-Bogdanovic, A. Jovic, B.N. Vasiljevic, M. Milojevic-Rakic, M. Kragovic, D. Krajsnik, I. Holclajtner-Antunovic, V. Dondur, 12-Tungstophosphoric acid/BEA zeolite composites - characterization and application for pesticide removal, *Mater. Sci. Eng. B-Advanced Funct. Solid-State Mater.* 225 (2017) 60–67, <https://doi.org/10.1016/j.mseb.2017.08.011>.
- [95] M. Milojevic-Rakic, A. Janosevic, J. Krstic, B.N. Vasiljevic, V. Dondur, G. Ciric-Marjanovic, Polyaniline and its composites with zeolite ZSM-5 for efficient removal of glyphosate from aqueous solution, *Microporous Mesoporous Mater.* 180 (2013) 141–155, <https://doi.org/10.1016/j.micromeso.2013.06.025>.
- [96] J.C. Millare, B.A. Basilia, Nanobubbles from ethanol-water mixtures: generation and solute effects via solvent replacement method, *ChemistrySelect* 3 (2018) 9268–9275, <https://doi.org/10.1002/SLCT.201801504>.
- [97] D.G. Oakenfull, D.E. Fenwick, Effect of ethanol on hydrophobic interactions. Conductometric study of ion-pair formation by double-long-chain electrolytes, *J. Phys. Chem.* 78 (1974) 1759–1763, https://doi.org/10.1021/J100610A018/ASSET/J100610A018.FP.PNG_V03.
- [98] L. Gong, F. Wu, W. Yang, C. Huang, W. Li, X. Wang, J. Wang, T. Tang, H. Zeng, Unraveling the hydrophobic interaction mechanisms of hydrocarbon and fluorinated surfaces, *J. Colloid Interface Sci.* 635 (2023) 273–283, <https://doi.org/10.1016/J.JCIS.2022.12.084>.
- [99] D. Ballal, W.G. Chapman, Hydrophobic and hydrophilic interactions in aqueous mixtures of alcohols at a hydrophobic surface, *J. Chem. Phys.* 139 (2013), 114706, <https://doi.org/10.1063/1.4821604>.
- [100] M.Z. Momcilovic, M.S. Radelovic, A.R. Zarubica, A.E. Onjia, M. Kokunesoski, B.Z. Matovic, SBA-15 templated mesoporous carbons for 2,4-dichlorophenoxyacetic acid removal, *Chem. Eng. J.* 220 (2013) 276–283, <https://doi.org/10.1016/j.cej.2012.12.024>.
- [101] J. Ortiz Otalvaro, M. Avena, M. Brigante, Adsorption of organic pollutants by amine functionalized mesoporous silica in aqueous solution. Effects of pH, ionic strength and some consequences of APTES stability, *J. Environ. Chem. Eng.* 7 (2019), <https://doi.org/10.1016/j.jece.2019.103325>.
- [102] I.P.P. Cansado, P.A.M. Mourão, J.A.F.L. Gomes, V. Almodovar, Adsorption of MCPA, 2,4-D and diuron onto activated carbons from wood composites, *Ciência Tecnol. Dos Mater.* 29 (2017) e224–e228, <https://doi.org/10.1016/J.CTMAT.2016.07.005>.
- [103] M.C. Hermosín, R. Celis, G. Facenda, M.J. Carrizosa, J.J. Ortega-Calvo, J. Cornejo, Bioavailability of the herbicide 2,4-D formulated with organoclays, *Soil Biol. Biochem.* 38 (2006) 2117–2124, <https://doi.org/10.1016/J.SOILBIO.2006.01.032>.
- [104] M. Blachnio, A. Derylo-Marczewska, B. Charmas, M. Zienkiewicz-Strzalka, V. Bogatyrov, M. Galaburda, Activated carbon from agricultural wastes for adsorption of organic pollutants, *Molecules* 25 (2020) 5105, <https://doi.org/10.3390/MOLECULES25215105>, 25 (2020) 5105.
- [105] C.C. Santiago, M.A. Fernández, R.M. Torres Sánchez, Adsorption and Characterization of MCPA on DDTMA- and Raw-Montmorillonite: Surface Sites Involved, 2016, pp. 245–253, <https://doi.org/10.1080/03601234.2015.1120618>.
- [106] M. Kersten, D. Tunega, I. Georgieva, N. Vlasova, R. Branscheid, Adsorption of the herbicide 4-chloro-2-methylphenoxyacetic acid (MCPA) by goethite, *Environ. Sci. Technol.* 48 (2014) 11803–11810, https://doi.org/10.1021/ES502444C/SUPPL_FILE/ES502444C_SI_003.AVI.
- [107] V. Rizzi, J. Gubitosa, P. Fini, R. Romita, A. Agostiano, S. Nuzzo, P. Cosma, Commercial bentonite clay as low-cost and recyclable “natural” adsorbent for the Carbendazim removal/recover from water: overview on the adsorption process and preliminary photodegradation considerations, *Colloids Surfaces A Physicochem. Eng. Asp.* 602 (2020), 125060, <https://doi.org/10.1016/J.COLSURFA.2020.125060>.
- [108] G. Li, J. Li, W. Tan, M. Yang, H. Wang, X. Wang, Effectiveness and mechanisms of the adsorption of carbendazim from wastewater onto commercial activated carbon, *Chemosphere* 304 (2022), 135231, <https://doi.org/10.1016/J.CHEMOSPHERE.2022.135231>.
- [109] A.A. Esquerdo, D.P. Rico, P.J.V. Galvañ, I.S. Gadea, Activated carbon and ozone to reduce simazine in water, *Water* 12 (2020) 2900, <https://doi.org/10.3390/W12102900>, 12 (2020) 2900.
- [110] F. Sannino, M.T. Filazzola, A. Violante, L. Gianfreda, Adsorption-desorption of simazine on montmorillonite coated by hydroxy aluminum species, *Environ. Sci. Technol.* 33 (1999) 4221–4225, <https://doi.org/10.1021/ES9813313/ASSET/IMAGES/LARGE/ES9813313F00003.JPG>.
- [111] B. Paul, D. Yang, X. Yang, X. Ke, R. Frost, H. Zhu, Adsorption of the herbicide simazine on moderately acid-activated beidellite, *Appl. Clay Sci.* 49 (2010) 80–83, <https://doi.org/10.1016/J.CLAY.2010.04.004>.
- [112] F. Sannino, S. Ruocco, A. Marocco, S. Esposito, M. Pansini, Simazine removal from waters by adsorption on porous silicas tailored by sol-gel technique, *Microporous Mesoporous Mater.* 180 (2013) 178–186, <https://doi.org/10.1016/J.MICROMESO.2013.06.026>.